
Asynchronous Heavy-Tailed Optimization

Junfei Sun¹ Dixi Yao¹ Xuchen Gong¹ Tahseen Rabbani¹ Manzil Zaheer² Tian Li¹

Abstract

Heavy-tailed stochastic gradient noise, commonly observed in transformer models, can destabilize the optimization process. Recent works mainly focus on developing and understanding approaches to address heavy-tailed noise in the centralized or distributed, *synchronous* setting, leaving the interactions between such noise and *asynchronous* optimization underexplored. In this work, we investigate two communication schemes that handle stragglers with asynchronous updates in the presence of heavy-tailed gradient noise. We propose and theoretically analyze algorithmic modifications based on delay-aware learning rate scheduling and delay compensation to enhance the performance of asynchronous algorithms. Our convergence guarantees under heavy-tailed noise match the rate of the synchronous counterparts and improve delay tolerance compared with existing asynchronous approaches. Empirically, our approaches outperform prior synchronous and asynchronous methods in terms of accuracy/runtime trade-offs and are more robust to hyperparameters in both image and language tasks.

1. Introduction

In stochastic optimization, heavy-tailed stochastic gradient noise is known to destabilize convergence or even cause divergence both empirically and theoretically (e.g., Zhang et al., 2020; Chezhegov et al., 2024). They are commonly observed in transformer models that currently dominate the state-of-the-art model architectures for language and vision tasks. Given the scale of modern datasets and transformer-based models, they are usually optimized (pre-trained or fine-tuned) in a distributed fashion by default. There is recent interest in various algorithmic developments for addressing the negative impacts of heavy-tailed noise in distributed, *synchronous* settings (Lee et al., 2025), where the

progress of worker¹ nodes are aggregated to update the global model.

Due to the inherently heterogeneous nature of large-scale training infrastructure (e.g., *met*), asynchronous aggregation is a promising alternative to synchronous variants to handle stragglers or slow networks (Xie et al., 2019; Zheng et al., 2020). Hence, it has the potential to scale up model training at a much larger scale. However, it remains underexplored both empirically and theoretically how heavy-tailed noise interplays with asynchronous training, and whether prior clipping-based methods that are developed for synchronous settings can generalize to the asynchronous case. More broadly, it remains an open question on how to incorporate information from stale (i.e., delayed) workers to the global model, under heavy-tailed noise.

In this work, we investigate the general setting of asynchronous optimization under heavy-tailed noise. Our framework also allows worker nodes to apply multiple gradient steps locally and send accumulated models updates to the server node, instead of sending a one-step gradient immediately. We propose two techniques to enhance the performance of asynchronous heavy-tailed optimization. First, model updates from extreme stragglers are obtained from a stale snapshot of the model many rounds ago; hence, naively incorporating them into the current global model (maintained on the server node) is suboptimal. Instead of directly dropping the stale information, we perform delay-aware aggregation, softly rescaling the updates based on the amount of staleness during aggregation. Second, we explicitly recover fresh model updates (accumulated gradient updates) from stale ones sent by the slow clients as if there were no delay. Throughout our analysis and experiments, we consider the common *soft* setting for asynchronous optimization where each server-side update waits for M client updates ($1 \leq M \leq N$ where N is the total number of clients) (Nguyen et al., 2022). When $M = 1$, it reduces to the fully asynchronous case. We provide convergence guarantees of the proposed enhancements without assuming bounded gradient variance and show that our approach offers a better delay tolerance under heavy-tailed noise (we use ‘staleness’ and ‘delay’ interchangeably in this paper).

¹Throughout this paper, we use ‘worker’ and ‘client’ interchangeably.

¹University of Chicago ²Work done at Meta. Correspondence to: Junfei Sun <junfeisun@uchicago.edu>.

Contributions. Our contributions are summarized as follows. (1) We study the problem of client-centric and server-centric asynchronous training with heavy-tailed noise. We propose delay-aware downplaying and delay compensation strategies to better incorporate stale updates from stragglers. (2) Theoretically, we present the first convergence results for vanilla asynchronous training while considering local updates and heavy-tailed noise. Moreover, we provide convergence results of our proposed approach with improved dependencies on the amount of delay. (3) We empirically show that our method outperforms vanilla asynchronous learning in terms of accuracy/runtime tradeoffs as well as ease of hyperparameter tuning across benchmark datasets.

2. Related Work

Heavy-Tailed Optimization. Heavy-tailed stochastic gradient distributions have been demonstrated to destabilize the training process both empirically and theoretically (Gorbunov et al., 2020; Lee et al., 2025), and can often be addressed by variants of clipping-based approaches (Simsekli et al., 2019; Juditsky et al., 2019; Chezhegov et al., 2024). However, to the best of our knowledge, the effects of heavy-tailed gradients (e.g., with unbounded variance) have not been explored for asynchronous training, which is critical when the infrastructure has heterogeneous hardware or network capabilities. In this work, we empirically show that prior clipping-based method proposed to address heavy-tailed noise can benefit asynchronous training as well, via limiting the impact of updates from stragglers (Section 5). Furthermore, we propose additional strategies that are tailored to asynchronous settings and theoretically analyze their effects in conjunction with clipping optimizers.

Asynchronous Distributed Training. Asynchronous optimization with many variants and setups has been extensively studied in prior literature for decades (Recht et al., 2011; Dean et al., 2012; De Sa et al., 2015). To further hide communication in distributed environments, existing works have also studied asynchronous training with local updates, where worker nodes run multiple (instead of one) gradient steps before sending the updates (Nguyen et al., 2022; Xie et al., 2019; Liu et al., 2024). For the full generality of our method, throughout the paper, we consider frameworks with local optimization by default, which involve both *local (inner)* and *global (outer)* optimizers. Such a nested scheme has been used in other prior works on asynchronous training of (large language) models (Liu et al., 2024; Kim et al., 2025). (Kim et al., 2025) propose a hierarchical local SGD structure combined with asynchronous training. We differ from this work by proposing to incorporate staleness-aware downplaying and delay compensation modifications and address heavy-tailed noise. Delay compensation has appeared in prior asynchronous distributed SGD works (Zheng et al.,

2017; Wang et al., 2022; Guan et al., 2017), but it has not been adapted, analyzed, or evaluated in our setting. Our specific staleness-aware downplaying algorithms are different from existing ones that downweight stale updates (Wang et al., 2024a) and demonstrate theoretically-improved tolerance to extreme delays (Section 4).

Notations. Throughout the paper, we consider the optimization objective $F(x)$ for model parameters $x \in \mathbb{R}^d$. Here, $F(x) := \mathbb{E}[F(x, \xi)]$ where $\nabla F(x, \xi) := \nabla F(x) + \langle x, \xi \rangle$ represents the stochastic gradient with noise ξ . Importantly, we assume that the stochastic noise can be heavy-tailed, i.e., $\mathbb{E}[\|\xi_i\|^\alpha] \leq D^\alpha$ for some $D > 0$ and $\alpha \in (1, 2)$ for any $\xi_i \sim \mathcal{D}_i$. For notations, M is the asynchronous buffer size (server waiting for M client updates to make one global update), and N is the total number of clients. We use K to denote the number of local steps, \odot or $(\cdot)^{\odot 2}$ to denote element-wise multiplication.

3. Asynchronous Heavy-Tailed Optimization

In this section, we aim to establish algorithms that can deal with heavy-tailed noise under an asynchronous setting. On a high level, we propose an asynchronous framework that uses the clipping method to control the heavy-tailed noise and enables this framework to be aware of the delay of the updates introduced by the asynchrony of the training process, which consequently ensures that the algorithms obtain reasonable convergence guarantees under biases both from asynchrony and heavy-tailed noise.

Server- and Client-Centric Asynchronous Models.

First we establish two schemes for asynchronous learning. Following previous notation, let the prefixed number of client updates needed for each global update be denoted as M . We allow for each client to run local updates (as opposed to one iteration to compute gradients) and the server to aggregate the accumulated model updates sent by the clients, which is a *nested* optimization framework. To address heavy-tailed noise, we employ the state-of-the-art coordinate-wise clipping based optimizer on the client side when running local optimization (Lee et al., 2025). However, under an asynchronous setting, we need a way to incorporate updates sent by the clients at different times. To this end, we consider *server-centric* and *client-centric* frameworks.

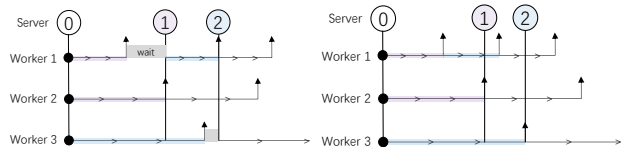


Figure 1. Illustrations of server- and client-centric asynchronous models where the total number of workers $N = 3$, number of local steps $K = 3$, and asynchronous buffer size $M = 2$.

Firstly, in the server-centric variant, the server proactively coordinates the learning process by sending global models to idle clients and updating the model whenever it receives M returned updates; while the clients passively wait for the server to send models. To be more specific, at any global round t , the server updates the global model x_{t-1} as soon as it has collected M clients updates. These M client updates may have different amounts of staleness, and we denote the local model from client i as $x_i^{\tau_{t,i}}$. $\tau_{t,i}$ denotes that the client model sent by client i and aggregated at global round t is a result of local optimization starting from a stale global model at time stamp $\tau_{t,i}$. In other words, client i runs local optimization from $x_{\tau_{t,i}}$ the update $x_i^{\tau_{t,i}} - x_{\tau_{t,i}}$ is used to obtain a global model x_t at the t -th global round.

On the contrary, in the client-centric case, every time a client sends its local model to the server, it will *immediately pull* the latest global model and perform the next update. This will result in a higher utilization rate of the clients, yet potentially making updates more biased by asynchrony. The pseudo-algorithm is summarized in Algorithm 1. *TailClip* denotes the clipping-based local optimizer with clipping threshold u_s (Lee et al., 2025), and *Outer_Optimizer* denotes any optimizer that the server uses to incorporate the

Algorithm 1: Vanilla server- and client-centric asynchronous learning

Input: Initial model x_0 , local learning rate schedule η_ℓ^t , clipping threshold $u_t \geq 0$, minimal number of model updates M ($1 \leq M \leq N$)

Server side: for $t = 1, \dots, T$ **do**

Collects first M client models $\{x_{i,K}\}_{i \in [M]}$ along with M time stamps
 Denotes the M time stamps as $\{\tau_{t,i}\}_{i \in [M]}$ and denotes $\{x_{i,K}\}_{i \in [M]}$ as $\{x_i^{\tau_{t,i}}\}_{i \in [M]}$
 $\Delta_t \leftarrow \frac{1}{M} \sum_{i \in [M]} (x_i^{\tau_{t,i}} - x_{\tau_{t,i}})$,
 $x_t \leftarrow \text{Outer_Optimizer}(x_{t-1}, \Delta_t)$
 Sets the current global model as x_t
 Sends x_t to idle clients /*only for server-centric*/

Client side: for each client i **in parallel do**

while *TRUE* **do**
 Waits to receive the latest global model (at global round s) from the server /*only for server-centric*/
 Pulls the latest global model from the server /*only for client-centric*/
 Sets the model to $x_{i,0}$
for each local step $k \in [K]$ **do**
 Draws gradient $g_{i,k} \leftarrow \nabla F(x_{i,k}; \xi_{i,k})$
 Runs inner optimization:
 $x_{i,k} \leftarrow x_{i,k-1} - \eta_\ell^t \cdot \text{TailClip}(u_s, g_{i,k})$
 Sends $x_{i,K}$ and s to the server

model updates Δ_t . For instance, it can perform clipping again on top of Δ_t before adding it to x_{t-1} . Figure 1 illustrates the differences between the two asynchrony schemes. Some previous asynchronous algorithms are similar to Algorithm 1 (Nguyen et al., 2022; Xie et al., 2019; Liu et al., 2021), but they do not consider or analyze clipping-based optimizers to handle heavy-tailed noise.

It is well-known that although an asynchronous training procedure can reduce the training time, the asynchrony inevitably introduces bias that comes from staleness, harming convergence: the gap between the historical global model that an update started from and the current global model. Therefore, besides simply incorporating asynchronous local updates from the clients, we should also propose new frameworks based on Algorithm 1 that actively deal with the bias introduced by asynchrony under heavy-tailed noise.

Staleness-Aware Downplaying and Delay Compensation.

In this part, for simplicity of presentation, we limit our discussion to the specific cases of Algorithm 1 where *Outer_Optimizer* is either simple averaging or *Clip*(\cdot); whereas inner optimizer is *Clip*(\cdot). Here *Clip* denotes coordinate-wise clipping that brings about the benefits of handling heavy-tailed noise and memory-efficient preconditioning (Lee et al., 2025). When the outer optimizer on the server side is simple average or does not apply any clipping operation, we name the base algorithm (Algorithm 1) as *SGDClip*. When the outer optimizer uses *Clip*(\cdot), we name the base algorithm as *Clip*².

Intuitively, one can consider downweighting the effects of delayed updates. Specifically, we adopt a dynamic outer learning $\eta/p_{t,i}$ for some constant η and $p_{t,i} := t - \tau_{t,i}$ being the delay for time t for client i , i.e., $\tau_{t,i}$ denoting the time stamp of the global model that client i starts with to obtain local updates $x_i^{\tau_{t,i}}$. We present the client-centric version of such a *staleness-aware downplaying (SD)* strategy in Algorithm 2 with blue highlight; the server-centric variant is similar. This indicates that we re-scale the updates sent to the server based on the amount of staleness, so that the bias in stale updates is controlled. We prove that we can tolerate larger delays for the convergence to hold compared with baselines (Section 4.2), and observe empirically that this delay-aware technique make the algorithm more robust to hyperparameter tuning (Section 5.2).

A potential downside of staleness-aware downplaying is that it may overlook useful information in the delayed updates. Hence, we propose a delay compensation (DC) technique aiming to approximate fresh model updates from the delayed ones (Algorithm 2 with red highlight). In particular, consider the first-order Taylor expansion of $\nabla F(x_{t-1})$ at $x_{\tau_{t,i}}$. To approximate the Hessian in such Taylor expansion cheaply, we use the product between the gradients at $x_{\tau_{t,i}}$.

As we consider multiple local updates, the clients sum up the Hessian approximators across all local iterations and send the statistics to the server, together with their model updates. Such a strategy is adapted from prior work (Zheng et al., 2020). Suppose at global round t , the server receives M updates $\{x_i^{\tau_{t,i}}\}_{i \in [M]}$ and Hessian approximators $\{A_i^{\tau_{t,i}}\}_{i \in [M]}$ (with initial global model $x_{\tau_{t,i}}$), the server-side aggregated model updates Δ_t would be corrected as

$$\Delta_t - \frac{1}{M} \sum_{i \in [M]} A_i^{\tau_{t,i}} \odot (x_{t-1} - x_{\tau_{t,i}}) \text{ where}$$

$$A_i^{\tau_{t,i}} \leftarrow \sum_{k=1}^K (\eta_\ell^{\tau_{t,i}})^2 (\text{Clip}(g_{i,k}) \odot \text{Clip}(g_{i,k})).$$

Here, $\eta_\ell^{\tau_{t,i}}$ is the local learning rate, $\text{Clip}(g_{i,k})$ denotes the clipped local stochastic gradients and \odot denotes the element-wise product.

We note that when $K = 1$ and $M = 1$, such updating rule reduces to the vanilla delay compensation studied in (Zheng et al., 2020). However, our update provably works for a distributed server-client nested optimization structure, and with the local updates taking multiple steps. Instead of downplaying the effect of delays like that in staleness-aware downplaying, the delay compensation framework incorporates an approximation to make the delayed update ‘fresher’. This way, even when there are clients that are consistently slow, the updates of the slow clients will not be ignored.

4. Convergence Analysis

In this section, we present some important convergence and delay-tolerance results of the frameworks that we proposed in section 3. The specific proofs are in Appendix B. Throughout this section, τ will be used to refer to the maximum delay throughout the training process, i.e., $\tau := \max_{t,i} \tau_{t,i}$. We also assume a bounded gradient of the target function F . This is a standard assumption necessary for the control of heavy-tailed noise in analysis, similarly done in relevant papers such as (Chezhegov et al., 2024), (Gorbunov et al., 2020), (Juditsky et al., 2019), (Lee et al., 2025), (Simsekli et al., 2019). A table summarizing the convergence guarantees of all our methods and comparing with other baselines is presented in Appendix A.

4.1. Vanilla Asynchronous Convergence Under Heavy-Tailed Noise

First of all, we present the first convergence results of vanilla server- and client-centric asynchronous framework under heavy-tailed noise (Algorithm 1). We show that under certain scheduling of client- and server-side clipping thresholds and learning rates, asynchronous *SGDClip* and *Clip*² converge with the same rates as the synchronous counterpart in

Algorithm 2: Proposed: *SGDClip/Clip*² with staleness-aware downplaying (SD) and *Clip*² with delay compensation (DC)

Input: Initial model x_0 , local learning rate schedule η_ℓ^t , global learning rate schedule η_t , local clipping threshold $u_t \geq 0$, global clipping threshold $\tilde{u}_t \geq 0$, minimal number of model updates M ($1 \leq M \leq N$)

Server side: for $t = 1, \dots, T$ **do**

Collects first M client models $\{x_{i,K}\}_{i \in [M]}$ along with M time stamps

Denotes the M time stamps as $\{\tau_{t,i}\}_{i \in [M]}$ and denotes $\{x_{i,K}\}_{i \in [M]}$ as $\{x_i^{\tau_{t,i}}\}_{i \in [M]}$

Collects the corresponding Hessian approximators

$\{A_{s,i}\}_{i \in [M]}$ and denotes them as $\{A_i^{\tau_{t,i}}\}_{i \in [M]}$

$p_{t,i} \leftarrow t - \tau_{t,i}, i \in [M]$

$\Delta_t \leftarrow \frac{1}{M} \sum_{i \in [M]} (x_i^{\tau_{t,i}} - x_{\tau_{t,i}}) / p_{t,i}$ (SD)
 $x_t \leftarrow x_{t-1} + \eta_t \Delta_t$ (*SGDClip* w/ SD)
 $x_t \leftarrow x_{t-1} + \eta_t \text{Clip}(\tilde{u}_t, \Delta_t)$ (*Clip*² w/ SD)

$\Delta_t \leftarrow \frac{1}{M} \sum_{i \in [M]} (x_i^{\tau_{t,i}} - x_{\tau_{t,i}})$

$\hat{g}_t \leftarrow \Delta_t - \frac{1}{M} \sum_{i \in [M]} A_i^{\tau_{t,i}} \odot (x_{t-1} - x_{\tau_{t,i}})$
 $x_t \leftarrow x_{t-1} + \eta_t \text{Clip}(\tilde{u}_t, \hat{g}_t)$ (*Clip*² w/ DC)

Sets the global model ready for pull as x_t

Client side: for each client i **in parallel do**

while *TRUE* **do**

Pulls the current global model (assuming at global round s) from the server and set as $x_{i,0}$

$A_{s,i} = 0$

for each local step $k \in [K]$ **do**

Draws gradient $g_{i,k} \leftarrow \nabla F(x_{i,k}; \xi_{i,k})$

Runs inner optimization:

$x_{i,k} \leftarrow x_{i,k-1} - \eta_\ell^s \cdot \text{Clip}(u_s, g_{i,k})$

$A_{s,i} \leftarrow A_{s,i} + (\eta_\ell^s)^2 (\text{Clip}(u_s, g_{i,k}) \odot \text{Clip}(u_s, g_{i,k}))$

Sends $x_{i,K}$, s , and $A_{s,i}$ to the server

(Lee et al., 2025), demonstrating reasonable delay tolerance, even with heavy-tailed noise. Specifically, when the stochastic noise satisfies that $\mathbb{E}[\|\xi\|^\alpha] \leq D^\alpha$ for $\alpha \in (1, 2)$, under mild assumptions, asynchronous *SGDClip* achieves

$$\min_{t \in [T]} \mathbb{E}[\|\nabla F(x_{t-1})\|^2] \leq O\left(T^{-\frac{\alpha-1}{2\alpha}}\right) \quad (1)$$

with a delay tolerance of maximum delay $\tau \leq O(T^{\frac{1}{2\alpha}})$. And asynchronous $Clip^2$ achieves

$$\min_{t \in [T]} \mathbb{E}[\|\nabla F(x_{t-1})\|^2] \leq O\left(T^{-\frac{\alpha-1}{4\alpha-2}}\right) \quad (2)$$

when $\tau \leq O(T^{\frac{\alpha}{4\alpha-2}})$. Due to space constraints, the formal statements and proofs are provided in Appendix B.1. Now, we move on to the analysis of our proposed delay-aware framework (Algorithm 2).

4.2. Staleness-Aware Downplaying

In this subsection, we will show that staleness-aware downplaying provides a softer delay restriction compared with vanilla $SGDClip$ or $Clip^2$ without it: Instead of being completely restricted by the maximum delay τ , staleness-aware downplaying makes the algorithm more tolerant to the maximum delay while still achieving convergence. We show in the following formal statements that without the need to assume a bounded delay, staleness-aware downplaying can achieve convergence as long as a certain proportion of clients have reasonable delay. All proofs for statements in this section are detailed in Appendix B.2.

4.2.1. $SGDClip$ WITH STALENESS-AWARE DOWNPLAYING

We first present results of $SGDClip$ (i.e., server-side optimizer being simple average and client-side optimizer being coordinate-wise clipping) with the proposed staleness-aware downplaying strategy.

Theorem 1. Assume $F(\cdot)$ being L -smooth and G -Lipschitz. Let u denote the client-side gradient clipping threshold and set it to $u = \Theta(T^\zeta)$, and let $p_{t,j}$ be the delay of the updates received at global round t for client j . If the stochastic gradient noise is heavy-tailed, i.e., it satisfies that $\mathbb{E}[\|\xi\|^\alpha] \leq D^\alpha$ for $\alpha \in (1, 2)$ and the delays satisfy $\sum_{t=1}^T \left(\sum_{j=1}^M \frac{1}{p_{t,j}}\right)^2 \geq \frac{2GM \sum_{t=1}^T \sum_{j=1}^M \frac{1}{p_{t,j}} \sum_{i=t-p_{t,j}}^{t-1} \frac{1}{p_{t,j}}}{Ku}$, $SGDClip$ with staleness-aware downplaying satisfies:

$$\begin{aligned} & \min_{t \in [T]} \mathbb{E}[\|\nabla F(x_{t-1})\|^2] \\ & \leq O\left(T^\zeta \frac{\sqrt{\sum_{t=1}^T \left(\sum_{j=1}^M \frac{1}{p_{t,j}}\right)^2}}{\sum_{t=1}^T \sum_{j=1}^M \frac{1}{p_{t,j}}} + T^{(1-\alpha)\zeta}\right). \end{aligned}$$

In particular, if all $p'_{t,j}$ s take the same value p , and $p = \Theta(T^b)$ with $b \leq \frac{1}{2\alpha}$, then setting $\zeta = \frac{1}{2\alpha}$ gives us

$$\min_{t \in [T]} \mathbb{E}[\|\nabla F(x_{t-1})\|^2] \leq O\left(T^{\frac{1-\alpha}{2\alpha}}\right).$$

Remark 1. We notice that when the delays are equal, we recover the same delay tolerance and the convergence guarantee as those of the vanilla asynchronous $SGDClip$. This is

expected since the introduction of $p_{t,j}$'s 'evens out' the bias of stale model updates. If the delays are uniform, then the bias does not require any evening out from the first place. However, the benefit of such a method is that it is less restrictive on delays when the delays are not uniform. To see this, we again turn our attention to the delay assumption in Theorem 1 above, and we notice that for this assumption to hold, it suffices to have

$$\sum_{t=1}^T \left(\sum_{j=1}^M \frac{1}{p_{t,j}}\right)^2 \geq \frac{2GM \sum_{t=1}^T \sum_{j=1}^M \frac{\sum_{i=t-p_{t,j}}^{t-1} 1}{p_{t,j}}}{Ku} = \frac{2GMT^2}{Ku}.$$

Now, we notice that with a fixed assignment of u , if we have very few very large $p_{t,j}$'s (larger than $O(T^{\frac{1}{2\alpha}})$), the equation can still hold since the value of $\sum_{t=1}^T \left(\sum_{j=1}^M \frac{1}{p_{t,j}}\right)^2$ is nearly the same. On the other hand, we can notice that for $SGDClip$ to achieve the bound in Eq. 1, we require that for every t, j , we have $p_{t,j} \leq \tau = O(T^{\frac{1}{2\alpha}})$.

Comparisons with Prior Work. There is prior work that studies a different way to perform staleness-aware downweighting for classic asynchronous optimization (Wang et al., 2024b). By the proof of Theorem 1, we can also obtain a more general bound that does not explicitly involve the requirement on the delays in Corollary 8. We now compare the bound in Corollary 8 with that in (Wang et al., 2024b). Firstly, the convergence in (Wang et al., 2024b) requires bounded variance, whereas our bound is valid even with heavy-tailed noise. Moreover, the convergence upper bound in prior work is determined by the average and median of the delays. If these values are large enough, the convergence bound explodes. However, a benefit of our convergence guarantee for $SGDClip$ with staleness-aware downplaying is that with a certain proportion of workers that have small enough delay, we can converge even when the median and average delays across all clients are large.

Proposition 1. If among all $p'_{t,j}$ s for $1 \leq t \leq T$, we have that there is $q \in (0, 1)$ fraction of delays that satisfies $p_{t,j} \leq A$ where $A \leq O(T^c)$, then when $c < \min\{\frac{1}{2} - \zeta, \frac{1}{4}\}$, we have that $SGDClip$ with staleness-aware downplaying converges. Or, if the minimum delay a_{\min} takes up a fixed fraction $p \in (0, 1)$ of all delays and satisfies $a_{\min} \leq O(T^{\frac{1}{2}})$, $SGDClip$ with staleness-aware downplaying also converges.

4.2.2. $Clip^2$ WITH STALENESS-AWARE DOWNPLAYING

Here we show that staleness-aware downplaying $Clip^2$ (i.e., both server- and client-side adopting coordinate-wise clipping) tolerates large (even unbounded) delays while still achieving convergence, similar to $SGDClip$.

Theorem 2. With the same assumption as in Theorem 1, \tilde{u} being the server-side clipping threshold, under the condition

$$\sqrt{\frac{C_1}{L \sum_{t=1}^T \left(\sum_{j=1}^M \frac{1}{p_{t,j}}\right)^2}} \leq \frac{2u\eta \sum_{t=1}^T \left(\sum_{j=1}^M \frac{1}{p_{t,j}}\right)}{(K+1) \sum_{t=1}^T \sum_{j=1}^M \frac{1}{p_{t,j}} \sum_{i=t-p_{t,j}}^{t-1} \frac{1}{p_{i,j}}},$$

if we let local learning rate $\eta_\ell = \Theta(T^\nu)$ and $\tilde{u} = \Theta(T^{\tilde{\zeta}})$, $Clip^2$ with staleness-aware downplaying achieves the convergence guarantee:

$$\min_{t \in [T]} \mathbb{E}[\|\nabla F(x_{t-1})\|^2] \leq O\left(T^{\tilde{\zeta}-\nu} \frac{\sqrt{\sum_{t=1}^T (\sum_{j=1}^M \frac{1}{p_{t,j}})^2}}{\sum_{t=1}^T (\sum_{j=1}^M \frac{1}{p_{t,j}})}\right) + T^{(1-\alpha)(\tilde{\zeta}-\nu)} + T^{(1-\alpha)\zeta} + T^{\zeta+\nu}.$$

In particular, if all $p'_{t,j}$ s take the same value p and $p = O(T^b)$ with $b \leq \frac{1}{4} + \frac{1}{4\alpha}$, we have

$$\min_{t \in [T]} \mathbb{E}[\|\nabla F(x_{t-1})\|^2] \leq O\left(T^{-\min\{\frac{3(\alpha-1)}{8}, \frac{\alpha-1}{4\alpha}\}}\right).$$

Similarly, for $Clip^2$, we can also obtain a bound that doesn't involve explicit requirements on the delays, presented in Corollary 11. Again, we have that this bound can converge even when the average and median delays are large, as long as we have a certain proportion of p'_t s being small enough:

Proposition 2. *If among all $p'_{t,j}$ s for $1 \leq t \leq T$, we have that there is $q \in (0, 1)$ fraction of delays that satisfies $p_{t,j} \leq A$ where $A \leq O(T^c)$, then when $c < \min\{\frac{1}{2} + \nu - \tilde{\zeta}, \frac{1}{4}\}$, we have that $Clip^2$ converges. Or, if the minimum delay a_{\min} takes up a fixed fraction $p \in (0, 1)$ of all delays and satisfies $a_{\min} \leq O(T^{\frac{1}{2}})$, we also have that $Clip^2$ converges.*

4.3. Delay Compensation

With the benefit of staleness-aware downplaying clarified theoretically, we move to analyze the convergence of delay compensation in Algorithm 2. We will show that $Clip^2$ with delay compensation is guaranteed to achieve the same convergence rate as the synchronous version. The delay tolerance is improved by a constant compared with vanilla asynchronous $Clip^2$. Note that the crucial difference in our setting is that the noise is heavy-tailed and we perform local updates so delay compensation is adapted. We have the following convergence result.

Theorem 3. *Assume F is μ -strongly convex in a ball centered at each local optimum x_{loc} with radius r ; F 's second and third order gradients are bounded; and satisfies $\|\mathbb{E}[(Clip(u_s, g_{i,k}))^{\odot 2}] - \mathbb{E}[Diag(H(x_{i,k}))]\| \leq O(1)\|x_{i,k} - x_{loc}\| + O(1)$ for any i, k . Running $Clip^2$ with delay compensation using the assignment $\omega = -\frac{1}{2}$, $\nu = -\frac{\alpha}{4\alpha-2}$, $\tilde{\zeta} = 0$, $\zeta = \frac{1}{4\alpha-2}$ gives us that when $\tau \leq O(T^{\frac{\alpha}{4\alpha-2}})$, we have*

$$\min_{t \in [T]} \|\nabla F(w_{t-1})\|^2 \leq O\left(T^{\frac{1-\alpha}{4\alpha-2}}\right).$$

Here we assume $\|\mathbb{E}[Clip(u_s, g_{i,k})^{\odot 2}] - \mathbb{E}[Diag(H(x_{i,k}))]\| \leq O(1)\|x_{i,k} - x_{loc}\| + O(1)$

for any s, i, k . $H(\cdot)$ is the Hessian of F and x_{loc} denotes any local optimum. This condition is necessary for Theorem 3 to hold. One way to satisfy this assumption is to consider a multi-class classification problem and let the loss function F be the expectation of per-sample cross-entropy loss as in (Zheng et al., 2020). We have the following remarks of our convergence results.

Remark 2. *$Clip^2$ with delay compensation achieve the same convergence guarantee with the same asymptotic delay tolerance as that of vanilla asynchronous $Clip^2$, which is $\tau \leq O(T^{\frac{1}{2}})$ (Appendix B.3). However, $Clip^2$ with delay compensation provides a constant improvement by $|1 - \eta_\ell^s|$ for delay tolerance. This can be seen by examining the constant factor of the restricting term for delay tolerance (the third to last term in Eq. (223) in Appendix B.3). But if we schedule η_ℓ^s to be decreasing as T increases, then the constant improvement decreases as T increases. This is because the compensation term is scaled by $(\eta_\ell^s)^2$, which makes the compensation effect smaller when η_ℓ^s is small.*

The complete convergence statements and proofs are in Appendix B.3. On a high level, the local step number K presents a tradeoff: as K increases, the primary convergence term is scaled down because of more local updates per step. However, a larger K leads to a larger drift error between the local model and the global model, which increases several terms in the rates (including the one associated with τ) and reduces the system's tolerance to delays. Similarly, the clipping thresholds also present a tradeoff on the convergence rates: certain terms increase as they increase as a result of the bias from heavy-tailed noise, yet other terms increase as they decrease, reflecting the loss of information from smaller clipping thresholds. Finally, the buffer size M primarily acts as an averaging mechanism for the convergence rates, it provides a variance reduction effect as the server averages updates from M different workers.

5. Experiments

In this section, we first evaluate the effects of vanilla server- and client-centric asynchronous training compared with synchronous variants (Section 5.1). We then demonstrate the benefits of our proposed staleness-aware downplaying and delay compensation techniques in Section 5.2, followed by additional studies on hyperparameters (Section 5.3). We assess the performance on a diverse set of empirical tasks. We study two different tasks: 1) image classification on the CIFAR-10 (Krizhevsky, 2009) dataset using a ViT model (Sharir et al., 2021), representing a standard computer vision workload; 2) natural language understanding on the GLUE benchmark (Wang, 2018) by fine-tuning a pre-trained BERT model (Devlin et al., 2018), which tests performance on popular transformer-based NLP tasks. We simulate two scenarios with *mild* and *large* delays for each

dataset. The specific experimental setup, runtime simulation, and hyperparameter tuning are laid out in Appendix C.

5.1. Benefits of Asynchronous Training under Heavy-Tailed Noise

In this section, we examine the performance of the proposed vanilla asynchronous training under heavy-tailed noise. Figure 2 shows the convergence results on CIFAR-10 and Table 1 demonstrates the final model performance on GLUE. We see that under heavy-tailed noise, asynchronous training could achieve competitive performance (similar accuracies while requiring much less runtime) compared with the synchronous counterpart for both client-centric (CC) and server-centric (SC) variants. The occurrence of large stragglers, however, may degrade performance compared with mild stragglers, given the bias introduced by larger delay. The final model performance and average runtime results are shown in Tables 8 and 9 in Appendix D.

Moreover, *Clip*², originally developed to handle heavy-tailed noise, has an inherent benefit of handling bias introduced by asynchrony (Figure 3). Additionally, we notice

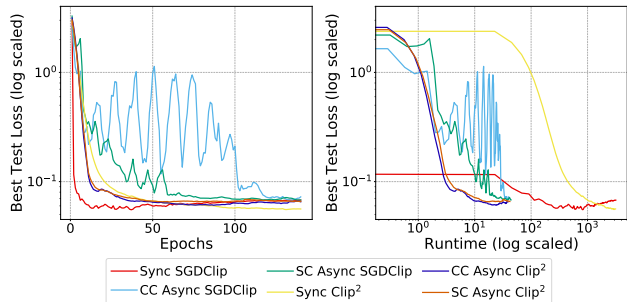


Figure 2. Test loss versus #epochs (left) and runtime (right) of synchronous SGDClip/*Clip*² and asynchronous SGDClip/*Clip*² with large stragglers. We observe that asynchronous methods provide similar loss as synchronous versions with significantly less runtime, across different optimizers including *Clip*² which is designed to handle heavy-tailed noise. Moreover, comparing ‘CC Async SGDClip’ with ‘CC Async *Clip*²’, (or ‘SC Async SGDClip’ with ‘SC Async *Clip*²’), we see that *Clip*² has inherent benefits to control the bias caused by asynchrony. We observe similar trends for the mild straggler setting (Figure 5 in the appendix).

that in Figure 2, vanilla asynchronous SGDClip introduces oscillations in the loss, which is caused by the bias from delays instead of the heavy-tailed noise, since there were no such oscillations under the synchronous setting. However, *Clip*² with a proper server-side clipping threshold effectively flattens those oscillations and converges.

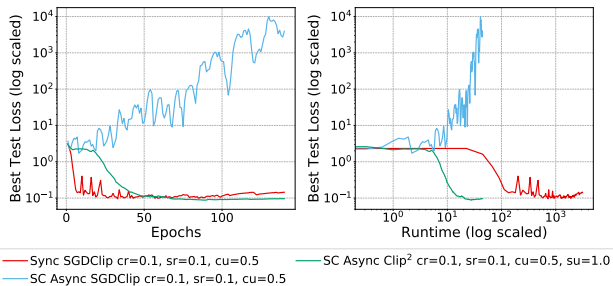


Figure 3. Test loss versus #epochs and runtime of Sync SGDClip, Async SGDClip and *Clip*² under a specific hyperparameter choice on CIFAR-10. ‘cr, sr, cu, su’ denotes client learning rate, server learning rate, client upper clipping bound, and server upper clipping bound, respectively. We see that vanilla asynchronous could cause divergence, whereas *Clip*², which is originally designed to handle heavy-tailed noise, can help convergence.

5.2. Effectiveness of Staleness-Aware Downplaying and Delay Compensation

In this part, we demonstrate the effectiveness of the two modifications we proposed (staleness-aware downplaying and delay compensation). Firstly, the average final model performance and runtime comparisons are presented in Table 8-Table 11 in Appendix D. In both datasets, we see that DC and SD can result in better best accuracies than vanilla asynchronous training. A subset of GLUE benchmark results are presented in Table 2. We see that under mild stragglers, DC notably improves RTE (+4.3) in the client-centric case. Under large stragglers, DC provides more consistent gains, improving MNLI, QNLI, and QQP. The runtime for all asynchronous training runs is similar for each dataset, and uniformly smaller than the synchronous counterpart (Table 14, Table 15, and Table 16).

	Async Mode	MNLI	QNLI	QQP	RTE	SST-2	MRPC	CoLA	STS-B	Avg
Mild Straggler	Sync	83.67	87.33	79.86	64.30	92.88	86.03	82.08	86.54	82.84
	Server	83.54	84.72	86.33	60.29	92.66	86.03	81.11	88.14	82.85
	Client	81.87	86.86	85.37	70.04	91.63	87.01	81.02	87.14	81.70
Large Straggler	Sync	83.30	87.22	83.03	64.30	92.78	85.05	79.77	86.43	81.45
	Server	82.58	85.78	86.09	59.95	91.97	83.58	80.44	85.63	82.00
	Client	82.19	86.89	85.39	67.87	92.29	85.05	80.15	86.92	81.33

Table 1. Comparison of synchronous training with vanilla server- and client-centric asynchronous training (Algorithm 1) on the GLUE benchmark. We see that under both mild and large delays, neither server-centric or client-centric variant degrades accuracies compared with the synchronous case, while greatly reducing the runtime (see Table 14 in the appendix). The optimizer is *Clip*².

Asynchronous Heavy-Tailed Optimization

	Async Mode	Methods	MNLI	QNLI	QQP	RTE	SST-2	MRPC	CoLA	STS-B	Avg
Mild Straggler	Server	vanilla	83.54	84.72	86.33	60.29	92.66	86.03	81.11	88.14	82.85
		SD	82.18	87.24	84.48	64.32	93.11	82.11	80.47	87.33	82.66
		DC	83.30	86.66	86.52	56.32	92.09	82.35	79.87	86.36	82.93
	Client	vanilla	81.87	86.86	85.37	70.04	91.63	87.01	81.02	87.14	81.70
		SD	83.42	86.91	86.10	70.76	92.20	85.78	80.35	86.19	84.00
		DC	81.56	86.53	86.57	70.40	92.09	86.76	81.88	88.37	84.27
Large Straggler	Server	vanilla	82.58	85.78	86.09	59.95	91.97	83.58	80.44	85.63	82.00
		SD	82.50	87.59	84.47	54.51	92.78	84.31	81.40	85.60	81.65
		DC	83.50	86.47	86.92	58.14	92.78	77.45	80.57	85.60	81.43
	Client	vanilla	82.19	86.89	85.39	67.87	92.29	85.05	80.15	86.92	81.33
		SD	83.35	86.55	86.96	72.56	91.51	86.52	80.73	86.60	84.35
		DC	82.29	86.36	84.44	66.43	91.63	86.03	81.78	87.91	83.36

Table 2. Comparison of results on GLUE for server- and client-centric training scenarios with and without staleness-aware downplaying (SD) and delay compensation (DC). The base optimizer is *Clip*². We see that SD or DC (Algorithm 2) improves over the vanilla asynchronous algorithm (Algorithm 1) in most cases.

In addition, on the CIFAR-10 dataset, we observe that for a large part of the hyperparameter choices in our sweep range that give non-converging loss curves for the vanilla asynchronous case, staleness-aware downplaying demonstrates converging behaviors instead. We present three specific hyperparameter choices that showcase this phenomenon in Figure 4. This shows that adding staleness-aware downplaying effectively makes the choice of hyperparameter more robust under an asynchronous setting with heavy-tailed noise. However, such a benefit is not evident for *Clip*² because, as we mentioned, all hyperparameter choices for vanilla asynchronous *Clip*² already give converging results.

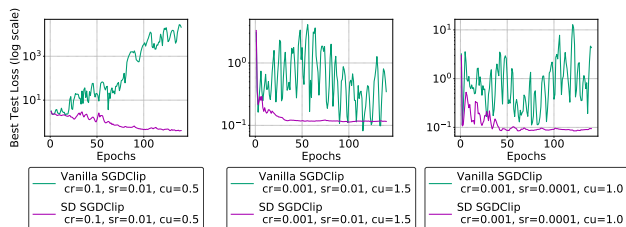


Figure 4. Test loss versus #epochs of vanilla asynchronous method and that with staleness-aware downplaying (SD) under SGDClip optimizer for three hyperparameter choices. SD largely improves the robustness of hyperparameter choosing.

Comparison with other Asynchronous Baselines. Our results show the effectiveness of our methods compared to vanilla asynchronous training and the synchronous baseline (Lee et al., 2025). In addition, we consider two asynchronous baselines: FADAS (Wang et al., 2024a), which uses client local SGD and a different server-side delay-aware aggregation with adaptive updates, and DN+DyLU (Liu et al., 2024), which performs delayed Nesterov (DN) for server aggregation and dynamic local updates (DyLU) with SGD. We can see that our proposed methods achieve higher accuracies compared to FADAS and DN+DyLU in Tables 12 and 17 in the appendix.

5.3. Additional Evaluation

Effects of M . We use M as the asynchronous buffer. When $M = 1$, the algorithm reduces to the extreme asynchronous version where the server-centric is equivalent to the client-centric variant. We examine the losses and runtimes for $M \in \{1, 10, 20, 30\}$. The specific results are in Appendix D.2. In general, we notice that changing from $M = 1$ to other values always improves the accuracy, whereas increasing M from 10 might not give better accuracy. On the other hand, the runtime always increases as M increases. But the runtime of asynchronous methods are always significantly lower than the synchronous method.

Effects of Server-Centric and Client-Centric Variants.

We study the effects of the two asynchronous mode—server- and client-centric settings in terms of loss and runtime. From the results in Appendix D.1, we notice that in general, server-centric methods provide similar accuracies in comparison to client-centric methods, but require slightly longer runtime, as expected, given that client-centric methods do not force the clients to wait, making it less time-consuming.

6. Conclusion

In this work, we have explored asynchronous distributed optimization under heavy-tailed noise. We have proposed two delay-aware strategies, staleness-aware downplaying and delay compensation, to improve final model performance and robustness to hyperparameters. We have analyzed the convergence behaviour of our framework under the general setup of heavy-tailed noise, local optimization, and clipped-based optimizers. We are able to achieve matching convergence rates as the synchronous counterpart and improved delay tolerances compared with other asynchronous approaches. We empirically validate the effectiveness of our approach on both image and text datasets.

Impact Statement

Our work aims to improve efficient distributed machine learning by developing general asynchronous algorithms in the presence of heavy-tailed noise. There are many potential societal consequences of our work depending on the applications at hand, none of which we feel must be specifically highlighted here.

References

- Building meta’s genai infrastructure. <https://engineering.fb.com/2024/03/12/data-center-engineering/building-metas-genai-infrastructure/>.
- Chezhegov, S., Klyukin, Y., ndrei Semenov, Beznosikov, A., Gasnikov, A., Horvath, S. S., Takac, M., and Gorbunov, E. Gradient clipping improves adagrad when the noise is heavy-tailed. *ArXiv*, 2024.
- De Sa, C. M., Zhang, C., Olukotun, K., and Ré, C. Taming the wild: A unified analysis of hogwild-style algorithms. *Advances in neural information processing systems*, 28, 2015.
- Dean, J., Corrado, G., Monga, R., Chen, K., Devin, M., Mao, M., Ranzato, M., Senior, A., Tucker, P., Yang, K., et al. Large scale distributed deep networks. *Advances in neural information processing systems*, 25, 2012.
- Devlin, J., Chang, M.-W., Lee, K., and Toutanova, K. Bert: Pre-training of deep bidirectional transformers for language understanding. *arXiv*, 2018.
- Gao, T., Fisch, A., and Chen, D. Making pre-trained language models better few-shot learners. *arXiv preprint arXiv:2012.15723*, 2020.
- Gorbunov, E., Danilova, M., and Gasnikov, A. Stochastic optimization with heavy-tailed noise via accelerated gradient clipping. *Advances in Neural Information Processing Systems*, 2020.
- Guan, N., Shan, L., Yang, C., Xu, W., and Zhang, M. Delay compensated asynchronous adam algorithm for deep neural networks. In *2017 IEEE International Symposium on Parallel and Distributed Processing with Applications and 2017 IEEE International Conference on Ubiquitous Computing and Communications (ISPA/IUCC)*, pp. 852–859. IEEE, 2017.
- Juditsky, A., Nazin, A., Nemirovsky, A., and Tsybakov, A. Algorithms of robust stochastic optimization based on mirror descent method. *Automation and Remote Control*, 80:1607–1627, 2019.
- Kim, G.-W., Li, J., Gandham, S., Baldonado, O., Gangidi, A., Balaji, P., Wang, Z., and Akella, A. Halos: Hierarchical asynchronous local sgd over slow networks for geo-distributed large language model training. *arXiv preprint arXiv:2506.04531*, 2025.
- Krizhevsky, A. Learning multiple layers of features from tiny images. 2009. URL <https://api.semanticscholar.org/CorpusID:18268744>.
- Lee, S. H., Zaheer, M., and Li, T. Efficient distributed optimization under heavy-tailed noise. *arXiv preprint arXiv:2502.04164*, 2025.
- Liu, B., Chhaparia, R., Douillard, A., Kale, S., Rusu, A. A., Shen, J., Szlam, A., and Ranzato, M. Asynchronous local-sgd training for language modeling. *arXiv preprint arXiv:2401.09135*, 2024.
- Liu, J., Xu, H., Wang, L., Xu, Y., Qian, C., Huang, J., and Huang, H. Adaptive asynchronous federated learning in resource-constrained edge computing. *IEEE Transactions on Mobile Computing*, 22(2):674–690, 2021.
- Malladi, S., Gao, T., Nichani, E., Damian, A., Lee, J. D., Chen, D., and Arora, S. Fine-tuning language models with just forward passes. *Advances in Neural Information Processing Systems*, 36:53038–53075, 2023.
- Nguyen, J., Malik, K., Zhan, H., Yousefpour, A., Rabbat, M., Malek, M., and Huba, D. Federated learning with buffered asynchronous aggregation. In *International conference on artificial intelligence and statistics*, pp. 3581–3607. PMLR, 2022.
- Raman, M., Maini, P., Kolter, J., Lipton, Z., and Pruthi, D. Model-tuning via prompts makes nlp models adversarially robust. arxiv. Technical report, Retrieved 2023-03-26, from <http://arxiv.org/abs/2303.07320>, 2023.
- Recht, B., Re, C., Wright, S., and Niu, F. Hogwild!: A lock-free approach to parallelizing stochastic gradient descent. *Advances in neural information processing systems*, 24, 2011.
- Sharir, G., Noy, A., and Zelnik-Manor, L. An image is worth 16x16 words, what is a video worth? *arXiv preprint arXiv:2103.13915*, 2021.
- Simsekli, U., Sagun, L., and Gurbuzbalaban, M. A tail-index analysis of stochastic gradient noise in deep neural networks. *International Conference on Machine Learning*, 2019.
- Wang, A. Glue: A multi-task benchmark and analysis platform for natural language understanding. *arXiv preprint arXiv:1804.07461*, 2018.

- Wang, H., Jiang, Z., Liu, C., Sarkar, S., Jiang, D., and Lee, Y. M. Asynchronous training schemes in distributed learning with time delay. *arXiv preprint arXiv:2208.13154*, 2022.
- Wang, Y., Wang, S., Lu, S., and Chen, J. Fadas: Towards federated adaptive asynchronous optimization. *arXiv preprint arXiv:2407.18365*, 2024a.
- Wang, Y., Wang, S., Lu, S., and Chen, J. Fadas: Towards federated adaptive asynchronous optimization, 2024b. URL <https://arxiv.org/abs/2407.18365>.
- Xie, C., Koyejo, S., and Gupta, I. Asynchronous federated optimization. *arXiv preprint arXiv:1903.03934*, 2019.
- Zhang, J., Karimireddy, S. P., Veit, A., Kim, S., Reddi, S., Kumar, S., and Sra, S. Why are adaptive methods good for attention models? *Advances in Neural Information Processing Systems*, 33:15383–15393, 2020.
- Zheng, S., Meng, Q., Wang, T., Chen, W., Yu, N., Ma, Z.-M., and Liu, T.-Y. Asynchronous stochastic gradient descent with delay compensation. In *International conference on machine learning*, pp. 4120–4129. PMLR, 2017.
- Zheng, S., Meng, Q., Wang, T., Chen, W., Yu, N., Ma, Z.-M., and Liu, T.-Y. Asynchronous stochastic gradient descent with delay compensation, 2020. URL <https://arxiv.org/abs/1609.08326>.

A. Convergence guarantees comparison table

Assumptions	Sync w/ local updates	Async w/ local updates	Dependence on the delay
Bounded variance Non-convex & smooth	$T^{-1/2}$	$O(T^{-1/2} + T^{-1}\tau\tau_{avg})$ (Wang et al., 2024a) $O(T^{-1/2})$ (Nguyen et al., 2022)	$O(\tau\tau_{avg})$ (Wang et al., 2024a) $\tau \leq O(T^{1/4})$ or $O(\tau^2)$ (Nguyen et al., 2022)
Heavy-tailed noise (unbounded variance) Non-convex & smooth	$T^{\frac{1-\alpha}{4\alpha-2}}$ (Lee et al., 2025)	This paper Vanilla async: SGDClip (Theorem 4): $T^{\frac{1-\alpha}{2\alpha}}$ Clip ² (Theorem 5): $T^{\frac{1-\alpha}{4\alpha-2}}$ Staleness-aware downplaying: SGDClip (Theorem 1): $T^{\frac{1-\alpha}{2\alpha}}$ Clip ² (Theorem 2): T^{-r} , where $r = \min\{\frac{3(\alpha-1)}{8}, \frac{\alpha-1}{4\alpha}\}$	This paper Vanilla async: SGDClip (Theorem 4): $\tau \leq O(T^{\frac{1}{2\alpha}})$ or $O(\tau)$ Clip ² (Theorem 5): $\tau \leq O(T^{\frac{1}{4\alpha-2}})$ or $O(\tau)$ Staleness-aware downplaying: SGDClip (Theorem 1): $\tau \leq \frac{1}{2\alpha}$; explicit dependence (Proposition 1): unrestricted by the largest delay Clip ² (Theorem 2): $\tau \leq \frac{1}{4} + \frac{1}{4\alpha}$; explicit dependence (Proposition 2): unrestricted by the largest delay
Heavy-tailed noise (unbounded variance) Strongly-convex	$T^{\frac{1-\alpha}{4\alpha-2}}$ (Lee et al., 2025)	This paper Non-convex results naturally carry over Additionally: Delay Compensation (Theorem 3): $T^{\frac{1-\alpha}{4\alpha-2}}$	This paper Non-convex results naturally carry over Additionally: Delay Compensation (Theorem 3): $\tau \leq O(T^{\frac{1}{2\alpha}})$; explicit dependence: $O(\tau)$, with a constant improvement of $\ 1 - \eta_\ell\ $ relative to vanilla

Table 3. Comparison of convergence rates and delay dependence for various optimization settings. This paper is the first to give explicit theoretical guarantees for asynchronous training under heavy-tailed noise. We see that all our methods achieve comparable convergence rates to the synchronous baseline (Lee et al., 2025) under certain delay tolerance. Moreover, staleness-aware downplaying possesses the benefit of converging even with unbounded delay, which is different from prior works (Wang et al., 2024a; Liu et al., 2024). Delay compensation achieves a constant improvement of $1 - \eta_\ell$ relative to vanilla asynchronous methods.

B. Complete Proofs

For the proofs in this section, we will simplify the setting and conduct all the analysis in this section with $M = 1$, given that a general M simply requires an additional averaging in the analysis and complicates notations. The analysis can be easily generalized.

B.1. SGDClip and Clip²

B.1.1. SGDClip

Theorem 4. Let $\eta_t = \Theta(t^\omega)$, $\eta_t^\ell = \Theta(t^\nu)$, $u_t = \Theta(t^\zeta)$. $\zeta > 0$, $\omega + \nu \geq -1$, $\omega \leq 0$. Assume smoothness of $F(\cdot)$ and the deterministic gradient $\nabla F(\cdot)$ is uniformly bounded by G . Assume the stochastic noise satisfies that $\mathbb{E}[\|\xi\|^\alpha] \leq D^\alpha$ for $\alpha \in (1, 2)$. Suppose we use Clip as the inner optimizer and SGD as the outer optimizer, we have that

$$\min_{t \in [T]} \mathbb{E}[\|\nabla F(x_{t-1})\|^2] \lesssim O\left(T^{2\zeta+\nu+\omega} + T^{(1-\alpha)\zeta} + T^{\nu+\zeta} + T^{\omega+\nu+\zeta} + \tau \cdot T^{2\omega+\nu+\zeta} + T^\gamma + \tau \cdot T^{-1-\omega-\nu}\right). \quad (3)$$

Proof. Following the update rule, we have that

$$x_t - x_{t-1} = -\eta_t \sum_{k=1}^K \eta_\ell^{\tau_t} \text{Clip}(u_{\tau_t}, \nabla F(x_k^{\tau_t}, \xi_k^{\tau_t})) := -\eta_t \bar{g}_t, \quad (4)$$

where τ_t is the time index for the model that source of the update for iteration t starts to optimize over, k is the local iteration, and $\xi_k^{\tau_t}$ is the heavy-tailed stochastic noise. We denote $\sum_{k=1}^K \eta_\ell^{\tau_t} \text{Clip}(u_{\tau_t}, \nabla F(x_k^{\tau_t}, \xi_k^{\tau_t}))$ as \bar{g}_t which is the pseudogradient. Due to L -smoothness of $F(\cdot)$:

$$F(x_t) \leq F(x_{t-1}) + \langle \nabla F(x_{t-1}), x_t - x_{t-1} \rangle + \frac{L}{2} \|x_t - x_{t-1}\|^2, \quad (5)$$

we have

$$F(x_t) \leq F(x_{t-1}) - \eta_t \langle \nabla F(x_{t-1}), \bar{g}_t \rangle + \eta_t^2 \frac{L}{2} \|\bar{g}_t\|^2 \quad (6)$$

$$= F(x_{t-1}) - \eta_t \left\langle \nabla F(x_{t-1}), \bar{g}_t - \sum_{k=1}^K \eta_\ell^{\tau_t} \nabla F(x_k^{\tau_t}, \xi_k^{\tau_t}) + \sum_{k=1}^K \eta_\ell^{\tau_t} \nabla F(x_k^{\tau_t}, \xi_k^{\tau_t}) \right\rangle \quad (7)$$

$$- \eta_t \langle \nabla F(x_{t-1}), -K \eta_\ell^{\tau_t} \nabla F(x_{t-1}) + K \eta_\ell^{\tau_t} \nabla F(x_{t-1}) \rangle + \eta_t^2 \frac{L}{2} \|\bar{g}_t\|^2 \quad (8)$$

$$= F(x_{t-1}) - \eta_t \underbrace{\left\langle \nabla F(x_{t-1}), \bar{g}_t - \sum_{k=1}^K \eta_\ell^{\tau_t} \nabla F(x_k^{\tau_t}, \xi_k^{\tau_t}) \right\rangle}_{A_1} + \eta_t^2 \frac{L}{2} \|\bar{g}_t\|^2 \quad (9)$$

$$- \eta_t \underbrace{\left\langle \nabla F(x_{t-1}), \sum_{k=1}^K \eta_\ell^{\tau_t} \nabla F(x_k^{\tau_t}, \xi_k^{\tau_t}) - K \eta_\ell^{\tau_t} \nabla F(x_{t-1}) \right\rangle}_{A_2} - K \eta_t \eta_\ell^{\tau_t} \|\nabla F(x_{t-1})\|^2. \quad (10)$$

Next, we would like to bound $\mathbb{E}[A_1]$ where the expectation is taken over all randomness so far. First, we have

$$\mathbb{E}[A_1] \leq \eta_t G \mathbb{E} \left[\left\| \bar{g}_t - \sum_{k=1}^K \eta_\ell^{\tau_t} \cdot \nabla F(x_k^{\tau_t}, \xi_k^{\tau_t}) \right\| \right] \quad (11)$$

$$= \eta_t G \mathbb{E} \left[\left\| \sum_{k=1}^K \eta_\ell^{\tau_t} \text{Clip}(u_{\tau_t}, \nabla F(x_k^{\tau_t}, \xi_k^{\tau_t})) - \sum_{k=1}^K \eta_\ell^{\tau_t} \nabla F(x_k^{\tau_t}, \xi_k^{\tau_t}) \right\| \right] \quad (12)$$

$$\leq \eta_t \eta_\ell^{\tau_t} G \sum_{k=1}^K \mathbb{E} [\|\text{Clip}(u_{\tau_t}, \nabla F(x_k^{\tau_t}, \xi_k^{\tau_t})) - \nabla F(x_k^{\tau_t}, \xi_k^{\tau_t})\|] \quad (13)$$

We consider Clip applied to the L_2 norm as opposed to each coordinate now. For coordinate-wise clipping, a constant regarding \sqrt{d} would be added to the bound. Use χ to denote the indicator function. Therefore,

$$\mathbb{E}[A_1] \leq \eta_t \eta_\ell^{\tau_t} G \sum_{k=1}^K \mathbb{E} [\|\text{Clip}(u_{\tau_t}, \nabla F(x_k^{\tau_t}, \xi_k^{\tau_t})) - \nabla F(x_k^{\tau_t}, \xi_k^{\tau_t})\|] \quad (14)$$

$$\leq \eta_t \eta_\ell^{\tau_t} G \sum_{k=1}^K \mathbb{E} [\chi(\|\nabla F(x_k^{\tau_t}, \xi_k^{\tau_t})\| \geq u_{\tau_t}) \cdot \|\nabla F(x_k^{\tau_t}, \xi_k^{\tau_t})\|] \quad (15)$$

$$\leq \eta_t \eta_\ell^{\tau_t} G \sum_{k=1}^K \left(\underbrace{\mathbb{E} [\chi(\|\nabla F(x_k^{\tau_t}, \xi_k^{\tau_t})\| \geq u_{\tau_t}) \cdot \|\nabla F(x_k^{\tau_t}, \xi_k^{\tau_t})\|]}_{B_1} \right), \quad (16)$$

where we note that

$$B_1 \leq \mathbb{E} [\chi(\|\nabla F(x_k^{\tau_t}, \xi_k^{\tau_t})\| \geq u_{\tau_t}) \cdot \|\nabla F(x_k^{\tau_t}, \xi_k^{\tau_t})\|^\alpha \cdot \|\nabla F(x_k^{\tau_t}, \xi_k^{\tau_t})\|^{1-\alpha}] \quad (17)$$

$$\leq \mathbb{E} [\chi(\|\nabla F(x_k^{\tau_t}, \xi_k^{\tau_t})\| \geq u_{\tau_t}) \cdot \|\nabla F(x_k^{\tau_t}, \xi_k^{\tau_t})\|^\alpha \cdot u_{\tau_t}^{1-\alpha}] \quad (18)$$

$$\leq 2^{\alpha-1} \cdot (G^\alpha + D^\alpha) \cdot u_{\tau_t}^{1-\alpha} \cdot \mathbb{P}(\|\nabla F(x_k^{\tau_t}, \xi_k^{\tau_t})\| \geq u_{\tau_t}), \quad (19)$$

where the last step uses the fact that

$$\mathbb{E} [\|\nabla F(x_k^{\tau_t}, \xi_k^{\tau_t})\|^\alpha] = \mathbb{E} [\|\nabla F(x_k^{\tau_t}) + \xi_k^{\tau_t}\|^\alpha] \leq 2^{\alpha-1} (G^\alpha + \mathbb{E} [\|\xi_k^{\tau_t}\|^\alpha]) \leq 2^{\alpha-1} (G^\alpha + D^\alpha) \quad (20)$$

for any $\alpha \in (1, 2)$.

Next we proceed to bound $\mathbb{E}[A_2]$. Take expectation with respect to x_{t-1} ,

$$\begin{aligned}
 \mathbb{E}[A_2] &= -\eta_t \mathbb{E} \left\langle \nabla F(x_{t-1}), \sum_{k=1}^K \eta_\ell^{\tau_t} \nabla F(x_k^{\tau_t}, \xi_k^{\tau_t}) - K \eta_\ell^{\tau_t} \nabla F(x_{t-1}, \xi_k^{\tau_t}) \right\rangle \\
 &\leq \eta_t G \sum_{k=1}^K \|\mathbb{E} [\eta_\ell^{\tau_t} \nabla F(x_k^{\tau_t}, \xi_k^{\tau_t}) - \eta_\ell^{\tau_t} \nabla F(x_{t-1}, \xi_k^{\tau_t})]\| \\
 &= \eta_t G \sum_{k=1}^K \|\mathbb{E} [\eta_\ell^{\tau_t} \nabla F(x_k^{\tau_t}, \xi_k^{\tau_t}) - \eta_\ell^{\tau_t} \nabla F(x_{t-1}, \xi_k^{\tau_t})]\| \\
 &\leq \eta_t G \sum_{k=1}^K \eta_\ell^{\tau_t} \|\mathbb{E} [\nabla F(x_k^{\tau_t}, \xi_k^{\tau_t}) - \nabla F(x_{t-1}, \xi_k^{\tau_t})]\| \\
 &\leq \eta_t G \sum_{k=1}^K \eta_\ell^{\tau_t} L \mathbb{E} [\|x_k^{\tau_t} - x_{t-1}\|],
 \end{aligned}$$

where in the last inequality, we used Jensen, convexity, and L -smoothness. We may further decompose by

$$\|x_k^{\tau_t} - x_{t-1}\| \leq \sum_{i=0}^{k-1} \|x_{i+1}^{\tau_t} - x_i^{\tau_t}\| + \sum_{i=\tau_t}^{t-1} \|x_i - x_{i-1}\| \quad (21)$$

$$= \sum_{i=0}^{k-1} \eta_\ell^{\tau_t} \|\text{Clip}(u_{\tau_t}, \nabla F(x_i^{\tau_t}, \xi_k^{\tau_t}))\| + \sum_{i=\tau_t}^{t-1} \eta_i \|\bar{g}_i\| \quad (22)$$

$$\leq \sum_{i=0}^{k-1} u_{\tau_t} \eta_\ell^{\tau_t} + \sum_{i=\tau_t}^{t-1} \eta_i \eta_\ell^{\tau_{C_i}} K u_{\tau_{C_i}}. \quad (23)$$

Take expectation with respect to all randomness and combine all terms,

$$\mathbb{E}[F(x_t)] \leq \mathbb{E}[F(x_{t-1})] + \frac{L}{2} K^2 u_{\tau_t}^2 (\eta_\ell^{\tau_t})^2 \eta_t^2 - K \eta_t \eta_\ell^{\tau_t} \mathbb{E}[\|\nabla F(x_{t-1})\|^2] \quad (24)$$

$$+ 2^{\alpha-1} \cdot \eta_t \eta_\ell^{\tau_t} K (G^\alpha + D^\alpha) \cdot u_{\tau_t}^{1-\alpha} \cdot \mathbb{P}(\|\nabla F(x_k^{\tau_t}, \xi_k^{\tau_t})\| \geq u_{\tau_t}) \quad (25)$$

$$+ \eta_t \eta_\ell^{\tau_t} GL \cdot \sum_{k=1}^K \sum_{i=0}^{k-1} u_{\tau_t} \eta_\ell^{\tau_t} + \eta_t \eta_\ell^{\tau_t} GL \cdot \sum_{k=1}^K \sum_{i=\tau_t}^{t-1} \eta_i \eta_\ell^{\tau_{C_i}} K u_{\tau_{C_i}}. \quad (26)$$

Using the telescope sum gives

$$K \sum_{t=1}^T \eta_t \eta_\ell^{\tau_t} \mathbb{E}[\|\nabla F(x_{t-1})\|^2] \quad (27)$$

$$\leq \mathbb{E}[F(x_0)] - \mathbb{E}[F(x_T)] + \frac{LK^2}{2} \left(\sum_{t=1}^T u_{\tau_t}^2 (\eta_\ell^{\tau_t})^2 \eta_t^2 \right) \quad (28)$$

$$+ 2^{\alpha-1} K (G^\alpha + D^\alpha) \sum_{t=1}^T \eta_t \eta_\ell^{\tau_t} u_{\tau_t}^{1-\alpha} \cdot \mathbb{P}(\|\nabla F(x_k^{\tau_t}, \xi_k^{\tau_t})\| \geq u_{\tau_t}) \quad (29)$$

$$+ \frac{GL(K-1)(K-2)}{2} \sum_{t=1}^T \eta_t \eta_\ell^{\tau_t} u_{\tau_t} \eta_\ell^{\tau_t} + GL \sum_{t=1}^T \eta_t \eta_\ell^{\tau_t} \sum_{k=1}^K \sum_{i=\tau_t}^{t-1} \eta_i \eta_\ell^{\tau_{C_i}} K u_{\tau_{C_i}}. \quad (30)$$

Recall that we denote the model updates aggregated at round t come from the global fetched at round τ_t . We have the assumption that

$$t - \tau \leq \tau_t \leq t - 1 \quad (31)$$

for any round t . There exist c_1 and c_2 such that

$$c_1 t \leq \tau_t \leq c_2 t, \quad (32)$$

where c_1 and c_2 are two constants. We have that the bound becomes

$$\min_{t \in [T]} \mathbb{E}[\|\nabla F(x_{t-1})\|^2] \sum_{\ell=1}^T \eta_t \eta_\ell^t \leq \sum_{\ell=1}^T \eta_t \eta_\ell^t \mathbb{E}[\|\nabla F(x_{t-1})\|^2] \quad (33)$$

$$\lesssim \mathcal{O}(1) + \sum_{t=1}^T u_t^2 (\eta_t^t)^2 \eta_t^2 + K(G^\alpha + M^\alpha) \sum_{t=1}^T \eta_t \eta_\ell^t u_t^{1-\alpha} + \sum_{t=1}^T \eta_t (\eta_\ell^t)^2 u_t \quad (34)$$

$$+ \sum_{t=1}^T \eta_t \eta_\ell^t \cdot \underbrace{\sum_{i=t-\tau}^{t-1} \eta_i \eta_\ell^i u_i}_{\lesssim \tau \eta_t \eta_\ell^t u_t}. \quad (35)$$

Let $\eta_t = \Theta(t^\omega)$, $\eta_t^\ell = \Theta(t^\nu)$, $d_t = \Theta(t^\gamma)$, $u_t = \Theta(t^\zeta)$, and $\zeta > 0$ and $\gamma < 0$, $\omega + \nu \geq -1$, $\omega \leq 0$, we have

$$\min_{t \in [T]} \mathbb{E}[\|\nabla F(x_{t-1})\|^2] \lesssim \mathcal{O}\left(T^{2\zeta+\nu+\omega} + T^{(1-\alpha)\zeta} + T^{\nu+\zeta} + T^{\omega+\nu+\zeta} + \tau \cdot T^{\omega+\nu+\zeta} + T^\gamma + T^{-1-\omega-\nu}\right). \quad (36)$$

□

We can let

$$\omega = -\frac{\beta}{\alpha+1}, \nu = -\frac{\beta\alpha}{\alpha+1}, \zeta = \frac{\beta}{\alpha+1}, \quad (37)$$

which we plug into the original bound and get that

$$\min_{t \in [T]} \mathbb{E}[\|\nabla F(x_{t-1})\|^2] \leq \mathcal{O}(3T^{\beta\frac{1-\alpha}{\alpha+1}} + \tau \cdot T^{\beta\frac{-\alpha}{\alpha+1}} + T^{-1+\beta}). \quad (38)$$

Therefore, if we require $\tau \leq \mathcal{O}(T^{\frac{\beta}{\alpha+1}})$, then we have that

$$\min_{t \in [T]} \mathbb{E}[\|\nabla F(x_{t-1})\|^2] \leq \mathcal{O}(T^{-r}) \quad (39)$$

where

$$r = \min\left\{\beta\frac{\alpha-1}{\alpha+1}, 1-\beta\right\}. \quad (40)$$

And by equating them, we find that we can achieve a maximum $r = \frac{\alpha-1}{2\alpha}$ when $\beta = \frac{\alpha+1}{2\alpha}$ with a delay tolerance of $\tau \leq \mathcal{O}(T^{\frac{1}{2\alpha}})$.

B.1.2. Clip²

Theorem 5. Let $\eta_t = \Theta(t^\omega)$, $\eta_t^\ell = \Theta(t^\nu)$, $u_t = \Theta(t^\zeta)$, $\tilde{u}_t = \Theta(t^{\tilde{\zeta}})$, $\tilde{\zeta}, \zeta > 0$, $\omega + \nu \geq -1$, $\omega, \nu \leq 0$. Assume smoothness of $F(\cdot)$ and the deterministic gradient $\nabla F(\cdot)$ is uniformly bounded by G . Assume the stochastic noise satisfies that $\mathbb{E}[\|\xi\|^\alpha] \leq D^\alpha$ for $\alpha \in (1, 2)$. Suppose we use Clip as both the inner optimizer the outer optimizer, we have that

$$\min_{t \in [T]} \mathbb{E}[\|\nabla F(x_{t-1})\|^2] \lesssim \mathcal{O}\left(T^{-\nu-\omega-1} + T^{\omega+2\tilde{\zeta}-\nu} + T^{(\alpha-1)(\nu-\tilde{\zeta})} + T^{(1-\alpha)\zeta} + T^{\nu+\zeta} + \tau \cdot T^{\omega+\tilde{\zeta}}\right). \quad (41)$$

Proof. Following the update rule, we have that

$$x_t - x_{t-1} = \eta_t \text{Clip}(\tilde{u}_t, \bar{g}_t) \quad (42)$$

where \bar{g}_t is defined in the proof of Theorem 1. Now, by L -smoothness, we have

$$\mathbb{E}[F(x_t) - F(x_{t-1})] \leq \langle \nabla F(x_{t-1}), \mathbb{E}[x_t - x_{t-1}] \rangle + \frac{L}{2} \mathbb{E}[\|x_t - x_{t-1}\|^2] \quad (43)$$

$$\leq \eta_t \underbrace{\langle \nabla F(x_{t-1}), \mathbb{E}[\text{Clip}(\tilde{u}_t, -\bar{g}_t)] \rangle}_{A_1} + \frac{L\eta_t^2}{2} \mathbb{E}[\|\text{Clip}(\tilde{u}_t, \bar{g}_t)\|^2]. \quad (44)$$

We now bound A_1 as the following:

$$A_1 = \langle \nabla F(x_{t-1}), \mathbb{E}[\text{Clip}(\tilde{u}_t, -\bar{g}_t) \pm \bar{g}_t] \mp \sum_{k=1}^K \eta_\ell^{\tau_t} \mathbb{E}[\nabla F(x_k^{\tau_t}, \xi_k^{\tau_t})] \mp K\eta_\ell^{\tau_t} \nabla F(x_{t-1}) \rangle \quad (45)$$

$$= \underbrace{-\langle \nabla F(x_{t-1}), \mathbb{E}[\text{Clip}(\tilde{u}_t, -\bar{g}_t) + \bar{g}_t] \rangle}_{B_1} - \underbrace{\langle \nabla F(x_{t-1}), -\sum_{k=1}^K \eta_\ell^{\tau_t} \mathbb{E}[\nabla F(x_k^{\tau_t}, \xi_k^{\tau_t})] - \mathbb{E}[\bar{g}_t] \rangle}_{B_2} \quad (46)$$

$$\underbrace{-\langle \nabla F(x_{t-1}), \sum_{k=1}^K \eta_\ell^{\tau_t} \mathbb{E}[\nabla F(x_k^{\tau_t}, \xi_k^{\tau_t})] - K\eta_\ell^{\tau_t} \nabla F(x_{t-1}) \rangle}_{B_3} - K\eta_\ell^{\tau_t} \|\nabla F(x_{t-1})\|^2. \quad (47)$$

Now, we will move on to bound B_1, B_2 and B_3 respectively. Before that, we will first bound $\mathbb{E}[\|\bar{g}_t\|^\alpha]$:

$$\mathbb{E}[\|\bar{g}_t\|^\alpha] = \mathbb{E} \left[\left\| \eta_\ell^{\tau_t} \sum_{k=1}^K \text{Clip}(u_{\tau_t}, \nabla F(x_k^{\tau_t}, \xi_k^{\tau_t})) \right\|^\alpha \right] \quad (48)$$

$$\leq (\eta_\ell^{\tau_t})^\alpha K^\alpha \mathbb{E} \left[\left\| \frac{1}{K} \sum_{k=1}^K \text{Clip}(u_{\tau_t}, \nabla F(x_k^{\tau_t}, \xi_k^{\tau_t})) \right\|^\alpha \right] \quad (49)$$

$$\leq (\eta_\ell^{\tau_t})^\alpha K^{\alpha-1} \sum_{k=1}^K \mathbb{E} [\|\text{Clip}(u_{\tau_t}, \nabla F(x_k^{\tau_t}, \xi_k^{\tau_t}))\|^\alpha] \quad (50)$$

$$\leq (\eta_\ell^{\tau_t})^\alpha K^{\alpha-1} \sum_{k=1}^K (\mathbb{E}[\|\nabla F(x_k^{\tau_t}, \xi_k^{\tau_t})\|^\alpha]) \quad (51)$$

$$\leq (\eta_\ell^{\tau_t})^\alpha K^{\alpha-1} \underbrace{\sum_{k=1}^K (\eta_\ell^{\tau_t})^\alpha K^{\alpha-1} \sum_{k=1}^K \mathbb{E}[\|\nabla F(x_k^{\tau_t}, \xi_k^{\tau_t})\|^\alpha]}_C \quad (52)$$

by applying convexity and Jensen. Now, we also notice that

$$C \leq (\eta_\ell^{\tau_t})^\alpha K^{\alpha-1} \sum_{k=1}^K 2^\alpha \mathbb{E} \left[\frac{\|\nabla F(x_k^{\tau_t})\|^\alpha}{2} + \frac{\|\xi_k^{\tau_t}\|^\alpha}{2} \right] \quad (53)$$

$$\leq (\eta_\ell^{\tau_t})^\alpha K^{\alpha-1} \sum_{k=1}^K 2^\alpha (G^\alpha + D^\alpha). \quad (54)$$

Now, we plug in this bound for C and get that

$$\mathbb{E}[\|\bar{g}_t\|^\alpha] \leq (\eta_\ell^{\tau_t})^\alpha (K^{\alpha-1} \sum_{k=1}^K 2^{\alpha-1} (G^\alpha + D^\alpha)) := (\eta_\ell^{\tau_t})^\alpha \tilde{D}. \quad (55)$$

Now we are ready to bound B_1 , B_2 and B_3 :

$$B_1 \leq \|\nabla F(x_{t-1})\| \|\mathbb{E}[\text{Clip}(\tilde{u}_t, -\bar{g}_t) + \bar{g}_t]\| \text{ (by Cauchy-Schwartz)} \quad (56)$$

$$\leq \|\nabla F(x_{t-1})\| \mathbb{E}[\|\text{Clip}(\tilde{u}_t, -\bar{g}_t) + \bar{g}_t\|] \quad (57)$$

$$\leq G \cdot \mathbb{E}[\chi(\|\bar{g}_t\| \geq \tilde{u}_t) \|\bar{g}_t\|^\alpha \|\bar{g}_t\|^{1-\alpha}] \text{ (by the definition of Clip)} \quad (58)$$

$$\leq G \cdot [\mathbb{P}(\|\bar{g}_t\| \geq \tilde{u}_t) \mathbb{E}[\|\bar{g}_t\|^\alpha] \mathbb{E}[\|\bar{g}_t\|^{1-\alpha}]] \quad (59)$$

$$\leq G \cdot [\mathbb{P}(\|\bar{g}_t\| \geq \tilde{u}_t) (\eta_\ell^{\tau_t})^\alpha \tilde{D} \tilde{u}_t^{1-\alpha}] \quad (60)$$

$$\leq G (\eta_\ell^{\tau_t})^\alpha \tilde{D} \tilde{u}_t^{1-\alpha} \quad (61)$$

where the second to last inequality follows from the bound for $\mathbb{E}[\|\bar{g}_t\|^\alpha]$ and also that when $\|\bar{g}_t\| \geq \tilde{u}_t$, we have $\tilde{u}_t^{1-\alpha} \geq \|\bar{g}_t\|^{1-\alpha}$ because $1 - \alpha < 0$.

We now bound B_2 :

$$B_2 \leq G \cdot \left\| \sum_{k=1}^K \eta_\ell^{\tau_t} \mathbb{E}[\nabla F(x_k^{\tau_t}, \xi_k^{\tau_t})] + \mathbb{E}[\bar{g}_t] \right\| \quad (62)$$

$$\leq G \cdot \mathbb{E}[\left\| \sum_{k=1}^K \eta_\ell^{\tau_t} \nabla F(x_k^{\tau_t}, \xi_k^{\tau_t}) + \bar{g}_t \right\|] \quad (63)$$

$$\leq G \eta_\ell^{\tau_t} \cdot \left\| \sum_{k=1}^K \mathbb{E}[\nabla F(x_k^{\tau_t}, \xi_k^{\tau_t}) + \text{Clip}(u_{\tau_t}, \nabla F(x_k^{\tau_t}, \xi_k^{\tau_t}))] \right\| \quad (64)$$

$$\leq G \eta_\ell^{\tau_t} \cdot \sum_{k=1}^K [\mathbb{P}(\|\nabla F(\dots)\| \geq u_{\tau_t}) u_{\tau_t}^{1-\alpha} 2^{\alpha-1} (G^\alpha + D^\alpha)] \quad (65)$$

$$\text{(by the same analysis as that for bounding } C \text{)} \quad (66)$$

$$\leq G \eta_\ell^{\tau_t} \cdot \sum_{k=1}^K [u_{\tau_t}^{1-\alpha} 2^{\alpha-1} (G^\alpha + D^\alpha)]. \quad (67)$$

Finally, we bound B_3 :

$$B_3 \leq \eta_\ell^{\tau_t} G \cdot \mathbb{E}[\left\| \sum_{k=1}^K (\nabla F(x_k^{\tau_t}, \xi_k^{\tau_t}) - \nabla F(x_{t-1})) \right\|] \quad (68)$$

$$\leq \eta_\ell^{\tau_t} GL \sum_{k=1}^K \mathbb{E}[\|x_k^{\tau_t} - x_{t-1}\|] \text{ (by } L\text{-smoothness)} \quad (69)$$

Here, we notice that we can bound $\mathbb{E}[\|x_k^{\tau_t} - x_{t-1}\|]$ as the following:

$$\|x_k^{\tau_t} - x_{t-1}\| \leq \sum_{i=0}^{k-1} \|x_{i+1}^{\tau_t} - x_i^{\tau_t}\| + \sum_{i=\tau_t}^{t-1} \|x_i - x_{i-1}\| \quad (70)$$

$$= \sum_{i=0}^{k-1} \eta_\ell^{\tau_t} \|\text{Clip}(u_{\tau_t}, \nabla F(x_k^{\tau_t}, \xi_k^{\tau_t}))\| + \sum_{i=\tau_t}^{t-1} \eta_i \|\text{Clip}(\tilde{u}_i, \bar{g}_i)\| \quad (71)$$

$$\leq \sum_{i=0}^{k-1} u_{\tau_t} \eta_\ell^{\tau_t} + \sum_{i=\tau_t}^{t-1} \eta_i \tilde{u}_i. \quad (72)$$

We can now plug this into the bound of B_3 above and get that

$$B_3 \leq \eta_\ell^{\tau_t} GL \sum_{k=1}^K \sum_{i=0}^{k-1} u_{\tau_t} \eta_\ell^{\tau_t} + \eta_\ell^{\tau_t} GL \sum_{k=1}^K \sum_{i=\tau_t}^{t-1} \eta_i \tilde{u}_i \quad (73)$$

Now, we combine the upper bounds of B_1, B_2 , and B_3 to obtain an upper bound for A_1 . In turn, this gives us that

$$\mathbb{E}[F(x_t) - F(x_{t-1})] \leq \frac{L\eta_t^2 \tilde{u}_t^2}{2} - K\eta_t^{\tau_t} \eta_t \|\nabla F(x_{t-1})\|^2 + G\eta_t \tilde{d}_t + G\eta_t (\eta_t^{\tau_t})^\alpha \tilde{D} \tilde{u}_t^{1-\alpha} \quad (74)$$

$$+ G\eta_t \eta_t^{\tau_t} \cdot \sum_{k=1}^K [d_{\tau_t} + u_{\tau_t}^{1-\alpha} 2^{\alpha-1} (G^\alpha + D^\alpha)] \quad (75)$$

$$+ \eta_t \eta_t^{\tau_t} GL \sum_{k=1}^K \sum_{i=0}^{k-1} u_{\tau_t} \eta_t^{\tau_t} + \eta_t \eta_t^{\tau_t} GL \sum_{k=1}^K \sum_{i=\tau_t}^{t-1} \eta_i \tilde{u}_i. \quad (76)$$

Then, by considering the telescope sum, we have that

$$\sum_{t \in [T]} K\eta_t^{\tau_t} \eta_t \mathbb{E}[\|\nabla F(x_{t-1})\|^2] \leq F(x_0) - \mathbb{E}[F(x_T)] + \sum_{t \in [T]} \left(\frac{L\eta_t^2 \tilde{u}_t^2}{2} + G\eta_t (\eta_t^{\tau_t})^\alpha \tilde{D} \tilde{u}_t^{1-\alpha} \right) \quad (77)$$

$$+ \sum_{t \in [T]} G\eta_t \eta_t^{\tau_t} \cdot \sum_{k=1}^K [u_{\tau_t}^{1-\alpha} 2^{\alpha-1} (G^\alpha + D^\alpha)] \quad (78)$$

$$+ \sum_{t \in [T]} \eta_t \eta_t^{\tau_t} GL \sum_{k=1}^K \sum_{i=0}^{k-1} u_{\tau_t} \eta_t^{\tau_t} + \sum_{t \in [T]} \eta_t \eta_t^{\tau_t} GL \sum_{k=1}^K \sum_{i=\tau_t}^{t-1} \eta_i \tilde{u}_i. \quad (79)$$

Now, we let $\eta_t = \Theta(t^\omega)$, $\eta_t^\ell = \Theta(t^\nu)$, $u_t = \Theta(t^\zeta)$, $\tilde{u}_t = \Theta(t^{\tilde{\zeta}})$. By the same procedure as that in the proof of Theorem 1, we can conclude that

$$\min_{t \in [T]} \mathbb{E}[\|\nabla F(x_{t-1})\|^2] \lesssim O\left(T^{-\nu-\omega-1} + T^{\omega+2\tilde{\zeta}-\nu} + T^{(\alpha-1)(\nu-\tilde{\zeta})} + T^{(1-\alpha)\zeta} + T^{\nu+\zeta} + \tau \cdot T^{\omega+\tilde{\zeta}}\right). \quad (80)$$

□

For instance, one valid assignment is

$$\omega = -\frac{3}{4} + \frac{1}{4\alpha}, \nu = -\frac{1}{2\alpha}, \tilde{\zeta} = 0, \zeta = \frac{1}{4\alpha}. \quad (81)$$

Under this assignment, we have that $r_1 = \frac{\alpha-1}{4\alpha}$, $r_2 = \frac{3}{4} + \frac{1}{2\alpha}$, $r_5 = \frac{\alpha-1}{2\alpha}$, $r_6 = \frac{\alpha-1}{4\alpha}$, $r_7 = \frac{1}{4\alpha}$. Moreover, if we require $\tau \leq O(T^{\frac{1}{2}})$, then we have that $\tau \cdot T^{\omega+\tilde{\zeta}} \leq O(T^{\frac{1}{2}} T^{-\frac{3}{4} + \frac{1}{4\alpha}}) = O(T^{\frac{1-\alpha}{4\alpha}})$.

This gives $\min_{t \in [T]} \mathbb{E}[\|\nabla F(x_{t-1})\|^2] \lesssim O(T^{-r})$ where

$$r = \frac{\alpha-1}{4\alpha}. \quad (82)$$

In particular, if we assume $\alpha \geq 1.5$, then with $\tilde{\epsilon}$ big enough, we have that $r = \frac{\alpha-1}{4\alpha}$, which achieves minimum value $\frac{1}{12}$ when $\alpha = 1.5$.

Another valid assignment is

$$\omega = -\frac{1}{2}, \nu = -\frac{\alpha}{4\alpha-2}, \tilde{\zeta} = 0, \zeta = \frac{1}{4\alpha-2}, \quad (83)$$

we have

$$\min_{t \in [T]} \|\nabla F(x_{t-1})\|^2 \leq O(T^{\frac{1-\alpha}{4\alpha-2}}). \quad (84)$$

And when $\alpha = 1.5$, we achieve $r = \frac{1}{8}$.

Another assignment where ω, ν don't have to use the information of α is the following:

$$\omega = -\frac{1}{2}, \nu = -\frac{1}{4}, \tilde{\zeta} = 0, \zeta = \frac{1}{4\alpha}. \quad (85)$$

It can be verified that this also gives $r = \frac{\alpha-1}{4\alpha}$. But with a slightly worse delay tolerance where $\tau \leq O(T^{\frac{1}{4} + \frac{1}{4\alpha}})$.

B.2. Staleness-Aware Downplaying

B.2.1. SGDClip with Staleness-Aware Downplaying

Theorem 6. Assuming $F(\cdot)$ being L -smooth and G -Lipschitz, let u denote the client-side upper-clipping threshold, p_t be the delay of the updated received at global round t , K be the client epoch, η be the server-side learning rate and η_ℓ be the client-side learning rate. If the stochastic noise satisfies that $\mathbb{E}[\|\xi\|^\alpha] \leq D^\alpha$ for $\alpha \in (1, 2)$, SGDClip with staleness-aware downplaying satisfies:

$$\min_{t \in [T]} \mathbb{E}[\|\nabla F(x_{t-1})\|^2] \leq \frac{2\sqrt{2C_1(\frac{L}{2}u^2 \sum_{t=1}^T (\sum_{j=1}^M \frac{1}{p_{t,j}})^2)}}{\sum_{t=1}^T \sum_{j=1}^M \frac{1}{p_{t,j}}} + 2^{\alpha-1}(G^\alpha + D^\alpha)u^{1-\alpha} + GL \frac{(K-1)(K-2)}{2K} \eta_\ell u. \quad (86)$$

where $C_1 = \mathbb{E}[F(x_0) - F(x_T)]$ if we have that

$$\sum_{t=1}^T \left(\sum_{j=1}^M \frac{1}{p_{t,j}} \right)^2 \geq \frac{2GM \sum_{t=1}^T \sum_{j=1}^M \frac{1}{p_{t,j}} \sum_{i=t-p_{t,j}}^{t-1} \frac{1}{p_{i,j}}}{Ku}. \quad (87)$$

Proof. Substituting η_t with $\frac{\eta}{p_t}$ into the last step of SGDClip convergence analysis, we have that

$$K \sum_{t=1}^T \frac{\eta}{p_t} \eta_\ell \mathbb{E}[\|\nabla F(x_{t-1})\|^2] \leq C_1 + \frac{LK^2}{2} \left(\sum_{t=1}^T u^2 \eta_\ell^2 \frac{\eta^2}{p_t^2} \right) + 2^{\alpha-1} K (G^\alpha + D^\alpha) \sum_{t=1}^T \frac{\eta}{p_t} \eta_\ell u^{1-\alpha} \quad (88)$$

$$+ GL \frac{(K-1)(K-2)}{2} \sum_{t=1}^T \frac{\eta}{p_t} \eta_\ell^2 u + GL \sum_{t=1}^T \frac{\eta}{p_t} \eta_\ell \sum_{k=1}^K \sum_{i=t-p_t}^{t-1} \frac{\eta}{p_i} \eta_\ell K u. \quad (89)$$

This implies

$$\min_{t \in [T]} \mathbb{E}[\|\nabla F(x_{t-1})\|^2] \leq \frac{C_1}{K \eta \eta_\ell \sum_{t=1}^T \frac{1}{p_t}} + \frac{\frac{LK}{2} (\sum_{t=1}^T u^2 \eta_\ell \frac{\eta}{p_t^2})}{\sum_{t=1}^T \frac{1}{p_t}} + 2^{\alpha-1} (G^\alpha + D^\alpha) u^{1-\alpha} \quad (90)$$

$$+ GL \frac{(K-1)(K-2)}{2K} \eta_\ell u + \frac{GLK \eta \eta_\ell u \sum_{t=1}^T \frac{1}{p_t} \sum_{i=t-p_t}^{t-1} \frac{1}{p_i}}{\sum_{t=1}^T \frac{1}{p_t}} \quad (91)$$

$$\leq \frac{\frac{C_1}{K \eta \eta_\ell} + \frac{LK}{2} (2 \sum_{t=1}^T u^2 \eta_\ell \frac{\eta}{p_t^2})}{\sum_{t=1}^T \frac{1}{p_t}} + 2^{\alpha-1} (G^\alpha + D^\alpha) u^{1-\alpha} + GL \frac{(K-1)(K-2)}{2K} \eta_\ell u \quad (92)$$

$$\text{(by assumption (87))} \quad (93)$$

$$(94)$$

Now, we simply let

$$\eta \eta_\ell = \sqrt{\frac{C_1}{LK^2 u^2 \sum_{t=1}^T \frac{1}{p_t^2}}}. \quad (95)$$

This gives us the bound in the statement. \square

The theorem above and the corollary below together give Theorem 1.

Corollary 7. If we let $u = \Theta(T^\zeta)$, then we have that SGDClip with staleness-aware downplaying satisfies

$$\min_{t \in [T]} \mathbb{E}[\|\nabla F(x_{t-1})\|^2] \leq O \left(T^\zeta \sqrt{\frac{\sum_{t=1}^T (\sum_{j=1}^M \frac{1}{p_{t,j}})^2}{\sum_{t=1}^T \sum_{j=1}^M \frac{1}{p_{t,j}}}} + T^{(1-\alpha)\zeta} \right). \quad (96)$$

In particular, if $p_{t,j}$ s are all the same value p , and we have $p = \Theta(T^b)$ with $b \leq \frac{1}{2\alpha}$, then setting $\zeta = \frac{1}{2\alpha}$ gives us that

$$\min_{t \in [T]} \mathbb{E}[\|\nabla F(x_{t-1})\|^2] \leq O(T^{\frac{1-\alpha}{2\alpha}}). \quad (97)$$

Proof. Say $u = \Theta(T^\zeta)$ and $\eta_\ell = \Theta(T^\nu)$ where $\zeta > 0, \nu < 0$, we notice that the terms in the bound in Theorem 1 gives

$$\min_{t \in [T]} \mathbb{E}[\|\nabla F(x_{t-1})\|^2] \leq O\left(T^\zeta \frac{\sqrt{\sum_{t=1}^T \frac{1}{p_t^2}}}{\sum_{t=1}^T \frac{1}{p_t}} + T^{(1-\alpha)\zeta} + T^{\zeta+\nu}\right). \quad (98)$$

We can set ν very small, so the last term doesn't matter. Moreover, if p_t 's are all constant, then what we have is that the bound is

$$\min_{t \in [T]} \mathbb{E}[\|\nabla F(x_{t-1})\|^2] \leq O(T^{\zeta-\frac{1}{2}} + T^{(1-\alpha)\zeta} + T^{\zeta+\nu}). \quad (99)$$

Equating $\zeta - \frac{1}{2}$ and $(1 - \alpha)\zeta$ gives us that we can achieve the best convergence bound when $\zeta = \frac{1}{2\alpha}$, which is $O(T^{\frac{1-\alpha}{2\alpha}})$. However, we also need to examine the assumption (87), we notice that if all $p_t = p$, then these requirements become

$$\frac{T}{p^2} \geq \frac{2GT}{pKu} \Leftrightarrow p = O(u) = O(T^{\frac{1}{2\alpha}}). \quad (100)$$

□

By the proof of Theorem 1, we also obtain the following corollary that gives a bound without explicit requirement on the delays:

Corollary 8. For F being L -smooth and G -Lipschitz, if we set $\eta\eta_\ell = \sqrt{\frac{2C_1M^2}{LK^2u^2 \sum_{t=1}^T (\sum_{j=1}^M \frac{1}{p_{t,j}})^2}}$, *SGDClip with staleness-aware downplaying* satisfies $\min_{t \in [T]} \mathbb{E}[\|\nabla F(x_{t-1})\|^2]$ is upper bounded by

$$\frac{2\sqrt{C_1(\frac{L}{2}u^2 \sum_{t=1}^T (\sum_{j=1}^M \frac{1}{p_{t,j}})^2)}}{\sum_{t=1}^T (\sum_{j=1}^M \frac{1}{p_{t,j}})} + 2^{\alpha-1}(G^\alpha + D^\alpha)u^{1-\alpha} + GL \frac{(K-1)(K-2)}{2K} \eta_\ell u + \frac{2GM\sqrt{LC_1} \sum_{t=1}^T \sum_{j=1}^M \frac{1}{p_{t,j}} \sum_{i=t-p_{t,j}}^{t-1} \frac{1}{p_{i,j}}}{\sum_{t=1}^T (\sum_{j=1}^M \frac{1}{p_{t,j}}) \sqrt{\sum_{t=1}^T (\sum_{j=1}^M \frac{1}{p_{t,j}})^2}}. \quad (101)$$

The following proposition is used to compare the bound in Corollary 8 and that of FADAS, which is

$$\frac{1}{\sum_{t=1}^T \eta_t} \sum_{t=1}^T \eta_t \mathbb{E}[\|\nabla f(\mathbf{x}_t)\|^2] \leq O\left(\frac{\sqrt{\mathcal{F}\sigma}}{\sqrt{TKM}} + \frac{\sqrt{\mathcal{F}\sigma_g}}{\sqrt{TM}} + \frac{\mathcal{F}G\tau_c}{T\sqrt{M}} + \frac{\mathcal{F}\tau_{\text{avg}}}{T} + \frac{\mathcal{F}(\tau_c^2 + \tau_c\tau_{\text{avg}})}{T}\right). \quad (102)$$

where $\mathcal{F} = F(x_0) - F^*$ for $F^* = \min_x F(x)$, τ_{avg} and τ_c are average delay and median delay respectively, and if we assume that each stochastic gradient is unbiased and has a local variance bounded by σ , and the loss function on each client has a global variance bound σ_g .

Proposition (1). If among all p_t 's for $1 \leq t \leq T$, we have that there is $q \in (0, 1)$ fraction of delays that satisfies $p_t \leq A$ where $A \leq O(T^c)$, then when

$$c < \min\left\{\frac{1}{2} - \zeta, \frac{1}{4}\right\}, \quad (103)$$

we have that *SGDClip* converges. Or, if the minimum delay a value obtains a fixed fraction $p \in (0, 1)$ and satisfies $a \leq O(T^{\frac{1}{2}})$, we also have that *SGDClip* converges.

Proof. Firstly, we notice that as long as we set ζ, ν properly, we can always guarantee the convergence of $2^{\alpha-1}(G^\alpha + D^\alpha)u^{1-\alpha}$ and $GL \frac{(K-1)(K-2)}{2K} \eta_\ell u$. Therefore, we focus on the remaining two terms. We first notice that

$$\frac{2\sqrt{C_1(\frac{L}{2}u^2 \sum_{t=1}^T \frac{1}{p_t^2})}}{\sum_{t=1}^T \frac{1}{p_t}} \leq O\left(T^\zeta \cdot \frac{\sqrt{(1-q)\frac{T}{A^2} + qT}}{q\frac{T}{A}}\right) \quad (104)$$

$$\leq O\left(T^\zeta \cdot \left(\frac{1}{\sqrt{T}} + \frac{A}{\sqrt{T}}\right)\right) \quad (105)$$

$$\leq O\left(T^{\zeta-\frac{1}{2}} + T^{\zeta+c-\frac{1}{2}}\right). \quad (106)$$

Therefore, to ensure that this term converges, we need

$$\zeta < \frac{1}{2}, c < \frac{1}{2} - \zeta. \quad (107)$$

For the other term, we notice that

$$\frac{2G\sqrt{LC_1} \frac{1}{\sqrt{\sum_{t=1}^T \frac{1}{p_t^2}} \sum_{t=1}^T \frac{1}{p_t} \sum_{i=t-p_t}^{t-1} \frac{1}{p_i}}}{\sum_{t=1}^T \frac{1}{p_t}} \leq O\left(\frac{T}{\sqrt{qT \frac{1}{A^2}} (qT \frac{1}{A})}\right) \leq O\left(\frac{A^2}{\sqrt{T}}\right) = O\left(T^{2c-\frac{1}{2}}\right). \quad (108)$$

where, for the first inequality, we used the fairly loose upper bound

$$\sum_{t=1}^T \frac{1}{p_t} \sum_{i=t-p_t}^{t-1} \frac{1}{p_i} \leq \sum_{t=1}^T \frac{1}{p_t} \sum_{i=t-p_t}^{t-1} 1 = T. \quad (109)$$

Therefore, to ensure that this term converges, we need $c < \frac{1}{4}$. The proof of the second half of the proposition is completely analogous. But with better control of

$$\sum_{t=1}^T \frac{1}{p_t} \sum_{i=t-p_t}^{t-1} \frac{1}{p_i} \leq \sum_{t=1}^T \frac{1}{p_t} \sum_{i=t-p_t}^{t-1} \frac{1}{a} = \frac{T}{a}. \quad (110)$$

□

B.2.2. $Clip^2$ WITH STALENESS-AWARE DOWNPLAYING

Theorem 9. *With the same assumption as in Theorem 1, \tilde{u} being the server-side upper-clipping threshold, under the condition $\sqrt{\frac{C_1}{L \sum_{t=1}^T (\sum_{j=1}^M \frac{1}{p_{t,j}})^2}} \leq \frac{2u\eta_\ell \sum_{t=1}^T (\sum_{j=1}^M \frac{1}{p_{t,j}})}{(K+1) \sum_{t=1}^T \sum_{j=1}^M \frac{1}{p_{t,j}} \sum_{i=t-p_{t,j}}^{t-1} \frac{1}{p_{i,j}}}$, $Clip^2$ with staleness-aware downplaying achieves the convergence guarantee:*

$$\min_{t \in [T]} \mathbb{E}[\|\nabla F(x_{t-1})\|^2] \leq \sqrt{\frac{C_1 L \tilde{u}^2 \sum_{t=1}^T (\sum_{j=1}^M \frac{1}{p_{t,j}})^2}{K^2 \eta_\ell^2}} + \frac{G \tilde{D} \tilde{u}^{1-\alpha} \eta_\ell^{\alpha-1}}{K} + G u^{1-\alpha} 2^{\alpha-1} (G^\alpha + D^\alpha) + GLK(K+1)u\eta_\ell. \quad (111)$$

Proof. Again, by substituting η_t with $\frac{\eta}{p_t}$ in the last step of the proof of convergence bound for $Clip^2$, we obtain that

$$\sum_{t=1}^T K \frac{\eta}{p_t} \eta_\ell \mathbb{E}[\|\nabla F(x_{t-1})\|^2] \leq C_1 + \sum_{t=1}^T \left(\frac{L \eta^2 \tilde{u}^2}{2 p_t^2} + G \frac{\eta}{p_t} \eta_\ell \tilde{D} \tilde{u}^{1-\alpha} \right) + \sum_{t=1}^T G \frac{\eta}{p_t} \eta_\ell K u^{1-\alpha} 2^{\alpha-1} (G^\alpha + D^\alpha) \quad (112)$$

$$+ \sum_{t=1}^T \frac{\eta}{p_t} \eta_\ell GL \frac{K(K+1)}{2} u \eta_\ell + \sum_{t=1}^T \frac{\eta}{p_t} \eta_\ell GL \sum_{k=1}^K \sum_{i=t-p_t}^{t-1} \frac{\eta}{p_i} \tilde{u}. \quad (113)$$

And this gives us

$$\min_{t \in [T]} \mathbb{E}[\|\nabla F(x_{t-1})\|^2] \leq \frac{C_1}{K \eta \eta_\ell \sum_{t=1}^T \frac{1}{p_t}} + \sum_{t=1}^T \frac{\frac{L \eta \tilde{u}^2}{2 p_t^2}}{K \eta_\ell \sum_{t=1}^T \frac{1}{p_t}} + \frac{G \eta_\ell^{\alpha-1} \tilde{D} \tilde{u}^{1-\alpha}}{K} + G u^{1-\alpha} 2^{\alpha-1} (G^\alpha + D^\alpha) \quad (114)$$

$$+ GL \frac{K(K+1)}{2} u \eta_\ell + \frac{\sum_{t=1}^T \frac{1}{p_t} GL \sum_{k=1}^K \sum_{i=t-p_t}^{t-1} \frac{\eta}{p_i} \tilde{u}}{\sum_{t=1}^T \frac{1}{p_t}} \quad (115)$$

$$\leq \frac{C_1}{K \eta \eta_\ell \sum_{t=1}^T \frac{1}{p_t}} + \frac{L \eta \tilde{u}^2 \sum_{t=1}^T \frac{1}{2 p_t^2}}{K \eta_\ell \sum_{t=1}^T \frac{1}{p_t}} + \frac{G \eta_\ell^{\alpha-1} \tilde{D} \tilde{u}^{1-\alpha}}{K} + G u^{1-\alpha} 2^{\alpha-1} (G^\alpha + D^\alpha) \quad (116)$$

$$+ 2GL \frac{K(K+1)}{2} u \eta_\ell \text{ (by the condition of delays in Theorem 9)}. \quad (117)$$

The last inequality follows from the observation that the condition of delays in Theorem 9 gives us that

$$GL \frac{K(K+1)}{2} u \eta_\ell \geq \frac{\sum_{t=1}^T \frac{1}{p_t} GL \sum_{k=1}^K \sum_{i=t-p_t}^{t-1} \frac{\eta}{p_i} \tilde{u}}{\sum_{t=1}^T \frac{1}{p_t}}. \quad (118)$$

Now, we simply pick

$$\eta = \sqrt{\frac{C_1}{L \tilde{u}^2 \sum_{t=1}^T \frac{1}{p_t^2}}} \quad (119)$$

to get the convergence bound in the statement. \square

The theorem above and the corollary below together give Theorem 2.

Corollary 10. *If we let $\eta_\ell = \Theta(T^\nu)$ and $\tilde{u} = \Theta(T^{\tilde{\zeta}})$, we have that*

$$\min_{t \in [T]} \mathbb{E}[\|\nabla F(x_{t-1})\|^2] \leq O \left(T^{\tilde{\zeta}-\nu} \frac{\sqrt{\sum_{t=1}^T (\sum_{j=1}^M \frac{1}{p_{t,j}})^2}}{\sum_{t=1}^T (\sum_{j=1}^M \frac{1}{p_{t,j}})} + T^{(1-\alpha)(\tilde{\zeta}-\nu)} + T^{(1-\alpha)\zeta} + T^{\zeta+\nu} \right). \quad (120)$$

In particular, if all $p'_{t,j}$ s are all of the same value p , and we have $p = O(T^b)$ with $b \leq \frac{1}{4} + \frac{1}{4\alpha}$, we have

$$\min_{t \in [T]} \mathbb{E}[\|\nabla F(x_{t-1})\|^2] \leq O(T^{-r}) \quad (121)$$

where $r = \min\{\frac{3(\alpha-1)}{8}, \frac{\alpha-1}{4\alpha}\}$.

Proof. By letting $\eta_\ell = \Theta(T^\nu)$ and $\tilde{u} = \Theta(T^{\tilde{\zeta}})$, we have that the bound in the above theorem becomes

$$\min_{t \in [T]} \mathbb{E}[\|\nabla F(x_{t-1})\|^2] \leq O \left(T^{\tilde{\zeta}-\nu} \frac{\sqrt{\sum_{t=1}^T \frac{1}{p_t^2}}}{\sum_{t=1}^T \frac{1}{p_t}} + T^{(1-\alpha)(\tilde{\zeta}-\nu)} + T^{(1-\alpha)\zeta} + T^{\zeta+\nu} \right). \quad (122)$$

Here, if all p'_t s are the same value p with $p = O(T^b)$, then the bound becomes

$$\min_{t \in [T]} \mathbb{E}[\|\nabla F(x_{t-1})\|^2] \leq O(T^{\tilde{\zeta}-\nu-\frac{1}{2}} + T^{(1-\alpha)(\tilde{\zeta}-\nu)} + T^{(1-\alpha)\zeta} + T^{\zeta+\nu}). \quad (123)$$

And by the assignment that $\nu = -\frac{1}{4}$, $\tilde{\zeta} = \frac{1}{8} - \tilde{\epsilon}$, $\zeta = \frac{1}{4\alpha}$, we have

$$\min_{t \in [T]} \mathbb{E}[\|\nabla F(x_{t-1})\|^2] \leq O(T^{-r}) \quad (124)$$

where

$$r = \min \left\{ (\alpha-1) \left(\frac{3}{8} - \tilde{\epsilon} \right), \frac{\alpha-1}{4\alpha} \right\}. \quad (125)$$

And we can manually check that with this assignment, the assumption condition in Theorem 2 means precisely $b \leq \frac{1+\alpha}{4\alpha}$. \square

By the proof of Theorem 2, we also can obtain a bound without explicit requirements for delays:

Corollary 11. *Clip² with staleness-aware downplaying achieves the convergence guarantee:*

$$\min_{t \in [T]} \mathbb{E}[\|\nabla F(x_{t-1})\|^2] \leq \sqrt{\frac{C_1 L \tilde{u}^2 \sum_{t=1}^T (\sum_{j=1}^M \frac{1}{p_{t,j}})^2}{K^2 \eta_\ell^2}} + \frac{G \eta_\ell^{\alpha-1} \tilde{D} \tilde{u}^{1-\alpha}}{K} + G u^{1-\alpha} 2^{\alpha-1} (G^\alpha + D^\alpha) \quad (126)$$

$$+ GL \frac{K(K+1)}{2} u \eta_\ell + \frac{GM \sqrt{2C_1} L K \sum_{t=1}^T \sum_{t=1}^T \sum_{j=1}^M \frac{1}{p_{t,j}} \sum_{i=t-p_{t,j}}^{t-1} \frac{1}{p_{i,j}}}{\sum_{t=1}^T (\sum_{j=1}^M \frac{1}{p_{t,j}}) \sqrt{\sum_{t=1}^T (\sum_{j=1}^M \frac{1}{p_{t,j}})^2}}. \quad (127)$$

B.3. Delay Compensation

Here, again, for notation simplicity, we assume the client buffer size $M = 1$. In other words, the server updates the global model whenever it receives a new model update from any single client. Our proofs extend naturally to $M > 1$.

Notations. Similar as main text, here we use $(\cdot)^{\odot 2}$ to denote $(\cdot) \odot (\cdot)$, where \odot is element-wise multiplication. For instance, $(\text{Clip}(u_t, g_k^t))^{\odot 2}$ represents $\text{Clip}(u_t, g_k^t) \odot \text{Clip}(u_t, g_k^t)$. With slight switch of notations, we use w instead of x as the model parameter. w_k^t denotes the local model at the k -th local step, starting from a global model w_t . The corresponding stochastic gradient evaluated at w_k^t is g_k^t .

Lemma 1. *Assume F is μ -strongly convex in any r -radius ball centered at each local optimum w_{loc} . Assume F 's second order gradient (maximum eigen value of Hessian) is bounded by L , and satisfies $\|\mathbb{E}[(\text{Clip}(u_t, g_k^t))^{\odot 2}] - \mathbb{E}[\text{Diag}(H(w_k^t))]\| \leq O(1)\|w_k^t - w_{loc}\| + O(1)$ for any k, t . If we set $\eta_t \equiv \Theta(T^\omega)$, $\eta_\ell^t \equiv \Theta(T^\nu)$, $u_t \equiv \Theta(T^\zeta)$, $\tilde{u}_t \equiv \Theta(T^{\tilde{\zeta}})$, let $\tilde{g}_k^t := \text{Clip}(g_k^t)$ then asynchronous Clip^2 with delay compensation satisfies that for any t ,*

$$\|E[(\tilde{g}_k^t)^{\odot 2} - \text{Diag}(H(w_k^t))]\| \quad (128)$$

$$\leq O(T^{\nu+\zeta} + T^{\frac{(\alpha-1)\nu}{2}} + \tau^{\frac{\alpha}{2}} T^{\frac{(2\alpha-1)\nu+\alpha\omega+\alpha\zeta}{2}} + T^{\frac{\nu+\zeta}{2}} + \tau^{\frac{1}{2}} T^{\frac{\omega+\tilde{\zeta}}{2}} + \tau^{\frac{1}{2}} T^{\frac{2\zeta+\omega+\tilde{\zeta}+\nu}{2}} + T^{\frac{(1-\alpha)\zeta}{2}} + T^{\frac{\omega-\nu+2\tilde{\zeta}}{2}}) + \epsilon_{nc}. \quad (129)$$

Here we assume the local strong convexity of F , which is a weaker assumption than the typical global strong convexity assumption, and that allows us to cover more problem classes.

Proof. Denote $\text{Clip}(u_t, g_k^t)$ as \tilde{g}_k^t . By our assumption we have

$$\|E[(\tilde{g}_k^t)^{\odot 2} - \text{Diag}(H(w_k^t))]\| \leq O(1)\|w_k^t - w_{loc}\| + O(1). \quad (130)$$

Our goal now is to bound $\|w_t - w_{loc}\|$. We notice that for any t ,

$$\|w_k^t - w_{loc}\| \leq \|w_k^t - w_t\| + \|w_t - w_{loc}\| \quad (131)$$

$$\leq \left\| \sum_{i=1}^k \eta_\ell^t \text{Clip}(u_t, \nabla F(w_i^t) + \xi_i^t) \right\| + \|w_t - w_{loc}\| \quad (132)$$

$$\leq k\sqrt{d}\eta_\ell^t u_t + \|w_{t-1} - w_{loc}\|. \quad (133)$$

Suppose $w_t \in B_r(w_{loc})$ where $B_r(w_{loc})$ is the ball centering around some local optimum w_{loc} with radius r (we later show in B.3 that this is guaranteed to happen after a constant number of steps, i.e., $t \geq T_0$). With $w_t \in B_r(w_{loc})$, we have $\|w_t - w_{loc}\|^2 \leq \frac{2}{\mu} \|F(w_t) - F(w_{loc})\|$ by the assumption of local strong convexity. Therefore, it suffices to bound $F(w_t) - F(w_{loc})$. To do this, recall that $\bar{g}_t = \sum_{k=1}^K \eta_\ell^{\tau_t} \text{Clip}(u_{\tau_t}, \nabla F(w_k^{\tau_t}, \xi_k^{\tau_t}))$ we see that

$$\mathbb{E}[F(w_t)] - F(w_{loc}) \quad (134)$$

$$\leq F(w_{t-1}) - F(w_{loc}) - \eta_t \langle \nabla F(w_{t-1}), \mathbb{E}[\text{Clip}(\tilde{u}_t, -\bar{g}_t)] \rangle + \frac{L\eta_t^2 \|\mathbb{E}[\text{Clip}(\tilde{u}_t, -\bar{g}_t)]\|^2}{2} \quad (135)$$

$$\leq F(w_{t-1}) - F(w_{loc}) - K\eta_\ell^{\tau_t} \eta_t \|\nabla F(w_{t-1})\|^2 + \eta_t \langle \nabla F(w_{t-1}), K\eta_\ell^{\tau_t} \nabla F(w_{t-1}) - \mathbb{E}[\text{Clip}(\tilde{u}_t, -\bar{g}_t)] \rangle \quad (136)$$

$$+ \frac{L\eta_\ell^2 \tilde{u}_t^2}{2} \quad (137)$$

$$\leq \left(1 - \frac{2K\eta_\ell^{\tau_t} \mu^2 \eta_t}{L}\right) (F(w_{t-1}) - F(w_{loc})) + \eta_t \langle \nabla F(w_{t-1}), K\eta_\ell^{\tau_t} \nabla F(w_{t-1}) - \mathbb{E}[\text{Clip}(\tilde{u}_t, -\bar{g}_t)] \rangle \quad (138)$$

$$+ \frac{L\eta_\ell^2 \tilde{u}_t^2}{2}. \quad (139)$$

Now, we notice that

$$\langle \nabla F(w_{t-1}), K\eta_\ell^{\tau_t} \nabla F(w_{t-1}) - \mathbb{E}[Clip(\tilde{u}_t, -\bar{g}_t)] \rangle \quad (140)$$

$$= \langle \nabla F(w_{t-1}), K\eta_\ell^{\tau_t} \nabla F(w_{t-1}) - \mathbb{E}[Clip(\tilde{u}_t, -\bar{g}_t)] \pm \mathbb{E}\bar{g}_t \pm \sum_{k=1}^K \eta_\ell^{\tau_t} \mathbb{E}[Clip(u_{\tau_t}, \nabla F(w_k^{\tau_t}) + \xi_k^{\tau_t})] \rangle \quad (141)$$

$$\mp \sum_{k=1}^K \eta_\ell^{\tau_t} \nabla F(w_k^{\tau_t}) \rangle \quad (\pm \text{ here is a shorthand for first adding and then subtracting}) \quad (142)$$

$$= \underbrace{\langle \nabla F(w_{t-1}), \mathbb{E}[-\bar{g}_t - Clip(\tilde{u}_t, -\bar{g}_t)] \rangle}_{C_1} + \underbrace{\langle \nabla F(w_{t-1}), \sum_{k=1}^K \eta_\ell^{\tau_t} (\nabla F(w_{t-1}) - \nabla F(w_k^{\tau_t})) \rangle}_{C_2} \quad (143)$$

$$+ \underbrace{\langle \nabla F(w_{t-1}), \sum_{k=1}^K \eta_\ell^{\tau_t} \mathbb{E}[Clip(u_{\tau_t}, \nabla F(w_k^{\tau_t}) + \xi_k^{\tau_t})] + \mathbb{E}[\bar{g}_t] \rangle}_{C_3} \quad (144)$$

$$+ \underbrace{\langle \nabla F(w_{t-1}), \sum_{k=1}^K \eta_\ell^{\tau_t} (\nabla F(w_k^{\tau_t})) - \mathbb{E}[Clip(u_{\tau_t}, \nabla F(w_k^{\tau_t}) + \xi_k^{\tau_t})] \rangle}_{C_4}. \quad (145)$$

Our task is now to bound all of them respectively. Firstly, for C_1 , we have that

$$C_1 \leq G \|\mathbb{E}[-\bar{g}_t - Clip(\tilde{u}_t, -\bar{g}_t)]\| \leq G [\mathbb{P}(\tilde{u}_t \leq \|\bar{g}_t\|) \|\bar{g}_t\|^\alpha \|\bar{g}_t\|^{1-\alpha}]. \quad (146)$$

And we have that

$$\mathbb{E}[\|\bar{g}_t\|^\alpha] = \mathbb{E}[\|\Delta_{\tau_t} - \sum_{k=1}^K (\eta_\ell^{\tau_t})^2 (\tilde{g}_k^{\tau_t} \odot \tilde{g}_k^{\tau_t}) \odot (w_{t-1} - w_{\tau_t})\|^\alpha] \quad (147)$$

$$\leq 2^\alpha \mathbb{E}[\underbrace{\|\Delta_{\tau_t}\|^\alpha}_{D_1} + \underbrace{\|\sum_{k=1}^K (\eta_\ell^{\tau_t})^2 (\tilde{g}_k^{\tau_t} \odot \tilde{g}_k^{\tau_t}) \odot (w_{t-1} - w_{\tau_t})\|^\alpha}_{D_2}]. \quad (148)$$

By what has been established in the proof of $Clip^2$, we have that $\mathbb{E}[D_1] \leq \frac{(\eta_\ell^{\tau_t-1})^\alpha}{2} \tilde{D}^\alpha$. And we have

$$\mathbb{E}[D_2] \leq \frac{1}{2} K^{\alpha-1} \eta_\ell^{2\alpha} \sum_{k=1}^K \mathbb{E}[\|\tilde{g}_k^{\tau_t} \odot \tilde{g}_k^{\tau_t} \odot (w_{t-1} - w_{\tau_t})\|^\alpha] \quad (149)$$

$$\leq \frac{1}{2} K^{\alpha-1} \eta_\ell^{2\alpha} \sum_{k=1}^K \mathbb{E}[\|\tilde{g}_k^{\tau_t}\|^{2\alpha} \|(w_{t-1} - w_{\tau_t})\|^\alpha] \quad (150)$$

$$\leq \frac{1}{2} K^{\alpha-1} \eta_\ell^{2\alpha} \sum_{k=1}^K 2^{2\alpha-2} (D^\alpha + D^\alpha)^2 \mathbb{E}[\|(w_{t-1} - w_{\tau_t})\|^\alpha] \quad (151)$$

$$\leq K^\alpha \eta_\ell^{2\alpha} 2^{2\alpha-3} (D^\alpha + D^\alpha)^2 (t - \tau_t)^{\alpha-1} \sum_{i=\tau_t}^{t-1} \eta_i^\alpha \tilde{u}_i^\alpha. \quad (152)$$

So we have that

$$C_1 \leq 2^{\alpha-1} (\eta_\ell^{\tau_t})^\alpha \tilde{D}^\alpha + K^\alpha \eta_\ell^{2\alpha} 2^{3\alpha-3} (D^\alpha + D^\alpha)^2 (t - \tau_t)^{\alpha-1} \sum_{i=\tau_t}^{t-1} \eta_i^\alpha \tilde{u}_i^\alpha. \quad (153)$$

Now, for C_2 , we have that

$$C_2 \leq G\eta_\ell L \sum_{k=1}^K \|w_{t-1} - w_k^{\tau_t}\| \quad (154)$$

$$\leq G\eta_\ell L \sum_{k=1}^K \left(\sum_{i=0}^{k-1} u_{\tau_t} \eta_\ell + \sum_{i=\tau_t}^{t-1} \eta_i \tilde{u}_i \right) \quad (155)$$

where the last inequality follows from telescoping similarly to the proof of Bi^2Clip . And for C_3 , we have

$$C_3 \leq G\eta_\ell^2 \|\tilde{g}_k^{\tau_t} \odot \tilde{g}_k^{\tau_t} \odot (w_{t-1} - w_{\tau_t})\| \quad (156)$$

$$\leq G\eta_\ell^2 du_{\tau_t}^2 \|w_{t-1} - w_{\tau_t}\| \quad (157)$$

$$\leq G\eta_\ell^2 du_{\tau_t}^2 \sum_{i=\tau_t}^{t-1} \eta_i \tilde{u}_i. \quad (158)$$

Finally, we bound C_4 :

$$C_4 \leq G\eta_\ell \sum_{k=1}^K \mathbb{E} \|\text{Clip}(u_{\tau_t}, \nabla F(w_k^{\tau_t}) + \xi_k^{\tau_t}) - (\nabla F(w_k^{\tau_t}) + \xi_k^{\tau_t})\| \quad (159)$$

$$\leq G\eta_\ell \sum_{k=1}^K \mathbb{E} \sqrt{\sum_{j=1}^d (\text{Clip}(u_{\tau_t}, \nabla F(w_k^{\tau_t}) + \xi_k^{\tau_t}) - (\nabla F(w_k^{\tau_t}) + \xi_k^{\tau_t}))_j^2} \quad (160)$$

$$\leq G\eta_\ell K du_{\tau_t}^{1-\alpha} 2^{\alpha-1} (D^\alpha + D^\alpha) \quad (161)$$

where the last inequality is because for any $1 \leq j \leq d$, we have

$$\mathbb{E}[(\text{Clip}(u_{\tau_t}, \nabla F(w_k^{\tau_t}) + \xi_k^{\tau_t}) - (\nabla F(w_k^{\tau_t}) + \xi_k^{\tau_t}))_j] \leq u_{\tau_t}^{1-\alpha} 2^{\alpha-1} (D^\alpha + D^\alpha). \quad (162)$$

Finally, let $\delta_t := \mathbb{E}[F(w_t)] - F(w_{loc})$, we combine these bounds with the asymptotic assignment and get that

$$\delta_t \leq (1 - \Theta(T^{\omega+\nu}))\delta_{t-1} + O(T^{\alpha\nu+\omega} + \tau^\alpha T^{2\alpha\nu+(\alpha+1)\omega+\alpha\tilde{\zeta}} + T^{\omega+2\nu+\zeta} + \tau T^{2\omega+\nu+\tilde{\zeta}} + \tau T^{2\zeta+2\omega+\tilde{\zeta}+2\nu} \quad (163)$$

$$+ T^{(1-\alpha)\zeta+\omega+\nu} + T^{2\omega+2\tilde{\zeta}}). \quad (164)$$

Notice that this should give a steady state:

$$\delta_t \sim \frac{O(T^{\alpha\nu+\omega} + \tau^\alpha T^{2\alpha\nu+(\alpha+1)\omega+\alpha\tilde{\zeta}} + T^{\omega+2\nu+\zeta} + \tau T^{2\omega+\nu+\tilde{\zeta}} + \tau T^{2\zeta+2\omega+\tilde{\zeta}+2\nu} + T^{(1-\alpha)\zeta+\omega+\nu} + T^{2\omega+2\tilde{\zeta}})}{\Theta(T^{\omega+\nu})} \quad (165)$$

$$= O(T^{(\alpha-1)\nu} + \tau^\alpha T^{(2\alpha-1)\nu+\alpha\omega+\alpha\tilde{\zeta}} + T^{\nu+\zeta} + \tau T^{\omega+\tilde{\zeta}} + \tau T^{2\zeta+\omega+\tilde{\zeta}+\nu} + T^{(1-\alpha)\zeta} + T^{\omega-\nu+2\tilde{\zeta}}). \quad (166)$$

And substituting this into Eq.(133), we have

$$\|w_k^t - w_{loc}\| \leq O(T^{\nu+\zeta}) + O(T^{\frac{(\alpha-1)\nu}{2}} + \tau^{\frac{\alpha}{2}} T^{\frac{(2\alpha-1)\nu+\alpha\omega+\alpha\tilde{\zeta}}{2}} + T^{\frac{\nu+\zeta}{2}} + \tau^{\frac{1}{2}} T^{\frac{\omega+\tilde{\zeta}}{2}} + \tau^{\frac{1}{2}} T^{\frac{2\zeta+\omega+\tilde{\zeta}+\nu}{2}} + T^{\frac{(1-\alpha)\zeta}{2}} + T^{\frac{\omega-\nu+2\tilde{\zeta}}{2}}). \quad (167)$$

Recall that we suppose $w_t \in B_r(w_{loc})$. Now we show that this indeed holds, by showing that if we run asynchronous $Clip^2$ for a constant number of steps, we can converge to a small value of the gradient. We know that

$$\mathbb{E}[F(w_t)] \leq F(w_{t-1}) - \eta_t \langle \nabla F(w_{t-1}), \mathbb{E}[\text{Clip}(\tilde{u}_t, -\bar{g}_t)] \pm \bar{g}_t \rangle + \frac{\eta_t^2 L \tilde{u}_t^2}{2} \quad (168)$$

$$= F(w_{t-1}) - \underbrace{\eta_t \langle \nabla F(w_{t-1}), \mathbb{E}[\text{Clip}(\tilde{u}_t, -\bar{g}_t)] + \bar{g}_t \rangle}_{B_1} - \underbrace{\eta_t \langle \nabla F(w_{t-1}), \mathbb{E}\bar{g}_t \rangle}_{B_2} + \frac{\eta_t^2 L \tilde{u}_t^2}{2}. \quad (169)$$

We notice that B_1 has the following bound by an identical argument to that of C_1 :

$$B_1 \leq G\eta_{t-1}[2^{\alpha-1}(\eta_\ell^{\tau_{t-1}})^\alpha \tilde{D}^\alpha + K^\alpha \eta_\ell^{2\alpha} 2^{3\alpha-3}(D^\alpha + D^\alpha)^2(t-1-\tau_{t-1})^{\alpha-1} \sum_{i=\tau_{t-1}}^{t-2} \eta_i^\alpha \tilde{u}_i^\alpha]. \quad (170)$$

Therefore, it remains to bound B_2 , we notice that

$$B_2 = \underbrace{-\eta_t \langle \nabla F(w_{t-1}), \mathbb{E} \Delta_{C_t} \rangle}_{T_1} - \underbrace{\eta_t \langle \nabla F(w_{t-1}), \mathbb{E} \sum_{k=1}^K (\eta_\ell^{\tau_t})^2 (\tilde{g}_k^{\tau_t})^{\odot 2} \odot (w_{t-1} - w_{\tau_t}) \rangle}_{T_2}. \quad (171)$$

The control of T_1 uses the same argument as that in $Clip^2$, which we will not repeat here. The resultant bound is

$$T_1 \leq G\eta_t \eta_\ell^{\tau_t} K u_{\tau_t}^{1-\alpha} 2^{\alpha-1} (G^\alpha + D^\alpha) + GL\eta_t \eta_\ell^{\tau_t} \sum_{k=1}^K \left(\sum_{i=0}^{k-1} u_{\tau_t} \eta_\ell^{\tau_t} + \sum_{i=\tau_t}^{t-1} \eta_i \tilde{u}_i \right) - K\eta_t \eta_\ell^{\tau_t} \|\nabla F(w_{t-1})\|^2. \quad (172)$$

Now, to control T_2 , we have that

$$T_2 \leq G\eta_t (\eta_\ell^{\tau_t})^2 \sum_{k=1}^K \|\mathbb{E}(\tilde{g}_k^{\tau_t})^{\odot 2} \odot (w_{t-1} - w_{\tau_t})\| \quad (173)$$

$$\leq G\eta_t (\eta_\ell^{\tau_t})^2 \sum_{k=1}^K u_{\tau_t}^2 \|w_{t-1} - w_{\tau_t}\| \quad (174)$$

$$\leq G\eta_t (\eta_\ell^{\tau_t})^2 K u_{\tau_t}^2 \sum_{i=\tau_t}^{t-1} \eta_i \tilde{u}_i. \quad (175)$$

Combining all these bounds together, we have that

$$K\eta_t \eta_\ell^{\tau_t} \|\nabla F(w_{t-1})\|^2 \quad (176)$$

$$\leq F(x_t) - \mathbb{E}F(x_{t-1}) + G\eta_t [2^{\alpha-1}(\eta_\ell^{\tau_{t-1}})^\alpha \tilde{D}^\alpha + K^\alpha \eta_\ell^{2\alpha} 2^{3\alpha-3}(D^\alpha + D^\alpha)^2(t-1-\tau_{t-1})^{\alpha-1} \sum_{i=\tau_{t-1}}^{t-2} \eta_i^\alpha \tilde{u}_i^\alpha] \quad (177)$$

$$+ G\eta_t \eta_\ell^{\tau_t} K u_{\tau_t}^{1-\alpha} 2^{\alpha-1} (G^\alpha + D^\alpha) + GL\eta_t \eta_\ell^{\tau_t} \sum_{k=1}^K \left(\sum_{i=0}^{k-1} u_{\tau_t} \eta_\ell^{\tau_t} + \sum_{i=\tau_t}^{t-1} \eta_i \tilde{u}_i \right) + G\eta_t (\eta_\ell^{\tau_t})^2 K u_{\tau_t}^2 \sum_{i=\tau_t}^{t-1} \eta_i \tilde{u}_i \quad (178)$$

$$+ \frac{L\eta_t \tilde{u}_t^2}{2}. \quad (179)$$

By the same telescoping argument as before, we obtain that

$$\min_{t \in [T]} \|\nabla F(w_{t-1})\|^2 \quad (180)$$

$$\leq O(T^{-\omega-\nu-1} + T^{(\alpha-1)(\nu-\tilde{\zeta})} + \tau^\alpha T^{\alpha\omega+\tilde{\zeta}+(2\alpha-1)\nu} + T^{(1-\alpha)\zeta} + T^{\nu+\zeta} + \tau T^{\tilde{\zeta}+\omega} + \tau T^{\omega+\nu+2\zeta+\tilde{\zeta}} + T^{2\tilde{\zeta}+\omega-\nu}). \quad (181)$$

Now, observe that if we assign

$$\omega = -\frac{1}{2}, \nu = -\frac{1}{4}, \tilde{\zeta} = \frac{1}{8} - \tilde{\epsilon}, \zeta = \frac{1}{4\alpha} \quad (182)$$

for some $\tilde{\epsilon} \in (0, \frac{1}{8})$, and for $\tau \leq O(T^b)$ where $b = \frac{3}{8} - \frac{1}{4\alpha} + \tilde{\epsilon}$, we can achieve

$$\min_{t \in [T]} \|\nabla F(w_{t-1})\|^2 \leq O(T^{\frac{1-\alpha}{4\alpha}}). \quad (183)$$

And this means after $T_0 \geq O(r^{-\frac{8\alpha}{\alpha-1}})$, we have that $\min_{t \in [T_0]} \|\nabla F(w_{t-1})\|^2 \leq L^2 r^2$. Similarly to Zheng et al. (2020), we assume without loss of generality that for $w_t \notin B_r(w_{loc})$ for some local minimum w_{loc} , we have that $\|\nabla F(x_t)\| \geq Lr$. Then we know that $\min_{t \in [T_0]} \|\nabla F(w_{t-1})\|^2 \leq L^2 r^2$ proves w_{T_0} entered $B_r(w_{loc})$.

Therefore, we can use Eq. (167) and conclude that

$$\|w_k^t - w_{loc}\| \leq O(T^{\nu+\zeta} + T^{\frac{(\alpha-1)\nu}{2}} + \tau^{\frac{\alpha}{2}} T^{\frac{(2\alpha-1)\nu+\alpha\omega+\alpha\zeta}{2}} + T^{\frac{\nu+\zeta}{2}} + \tau T^{\omega+\zeta} + \tau^{\frac{1}{2}} T^{\frac{2\zeta+\omega+\zeta+\nu}{2}} + T^{\frac{(1-\alpha)\zeta}{2}}). \quad (184)$$

since after T_0 , w_t will enter $B_r(w_{loc})$. And by Eq. (130), we have proven the lemma. \square

As we can see, the control of the error between $\mathbb{E}[(\tilde{g}_k^t)^{\odot 2}]$ and $\mathbb{E}[Diag(H(w_k^t))]$ in terms of the distance between the current model w_k^t and w_{loc} (which is a local optimal around which the loss function is strongly convex), i.e., $\|\mathbb{E}[(\tilde{g}_k^t)^{\odot 2}] - \mathbb{E}[Diag(H(w_k^t))]\| \leq O(1)\|w_k^t - w_{loc}\| + O(1)$, ensure that Eq. (130) in the proof of the Lemma holds, which will then enables the control of $T_{1,1}$ in Eq. 200 in the proof of the following Theorem. The key step for this deduction is that the likelihood function has the property that the expected value of the score function's derivative ratio is zero under the model's own distribution, i.e., $\mathbb{E}_{(y|x,w_t)}[\frac{\nabla^2(P(y|x,w_t))}{P(y|x,w_t)}] = 0$.

With this Lemma, we will prove the following theorem. And Theorem 3 follows directly.

Theorem 12. *In addition to the assumptions in Lemma 1, if we assume that for any w , we have $\|H(w) - Diag(H(w))\| \leq \epsilon_D$, and we have that F 's second order gradient is bounded by L , third order gradient is bounded by L' , then running Clip² with delay compensation gives us that*

$$\min_{t \in [T]} \|\nabla F(w_{t-1})\| \quad (185)$$

$$\leq O(T^{-\omega-\nu-1} + T^{(\alpha-1)\nu} + \tau^\alpha T^{\alpha\omega+(2\alpha-1)\nu+\alpha\zeta} + T^{(1-\alpha)\zeta} + T^{\omega-\nu+2\zeta} + \tau T^{(2-2\alpha)\zeta+\zeta+\omega+\nu} + \tau T^{\omega+2\nu+\zeta+\zeta} \quad (186)$$

$$+ \tau T^{\omega+\frac{(\alpha+1)\nu}{2}+\zeta} + \tau^{\frac{\alpha}{2}+1} T^{\frac{(2\alpha+1)\nu}{2}+(1+\frac{\alpha}{2})\omega+(1+\frac{\alpha}{2})\zeta} + \tau T^{\frac{3\nu+\zeta}{2}+\omega+\zeta} + \tau^{\frac{3}{2}} T^{\frac{2\zeta+3\omega+3\nu+3\zeta}{2}} + \tau T^{\frac{3\omega+\nu+4\zeta}{2}} + T^{\nu+\zeta} \quad (187)$$

$$+ \tau T^{\omega+\zeta} + \tau^2 T^{2\omega+2\zeta} + \tau T^{\omega+\zeta} + T^{3\nu+2\zeta}). \quad (188)$$

Proof. Again, by L -smoothness, we have that

$$\mathbb{E}F(w_t) \leq F(w_{t-1}) - \eta_t \langle \nabla F(w_{t-1}), \mathbb{E}Clip(\tilde{u}_t, -\bar{g}_t) \mp \bar{g}_t \mp \sum_{k=1}^K \eta_\ell^{\tau_t} [\nabla F(w_k^{\tau_t}) + \xi_k^{\tau_t} + H(w_k^{\tau_t})(w_{t-1} - w_{\tau_t})] \rangle \quad (189)$$

$$- \eta_t \langle \nabla F(w_{t-1}), \mp K \eta_\ell^{\tau_t} \nabla F(w_{t-1}) \rangle + \frac{L \eta_\ell^2 \|Clip(\tilde{u}_t, \bar{g}_t)\|^2}{2} \quad (190)$$

$$\leq F(w_{t-1}) - \underbrace{\eta_t \langle \nabla F(w_{t-1}), \mathbb{E}Clip(\tilde{u}_t, -\bar{g}_t) + \bar{g}_t \rangle}_{B_1} \quad (191)$$

$$- \underbrace{\eta_t \langle \nabla F(w_{t-1}), \sum_{k=1}^K \eta_\ell^{\tau_t} (Clip(u_{\tau_t}, \nabla F(w_k^{\tau_t}) + \xi_k^{\tau_t}) - (\nabla F(w_k^{\tau_t}) + \xi_k^{\tau_t})) \rangle}_{A_1} \quad (192)$$

$$- \underbrace{\eta_t \langle \nabla F(w_{t-1}), \mathbb{E} \sum_{k=1}^K (\eta_\ell^{\tau_t})^2 [(\tilde{g}_k^{\tau_t})^{\odot 2} \odot (w_{t-1} - w_{\tau_t}) - H(w_k^{\tau_t})(w_{t-1} - w_{\tau_t})] \rangle - K \eta_t \eta_\ell^{\tau_t} \|\nabla F(w_{t-1})\|^2}_{T_{1,1}} \quad (193)$$

$$+ \underbrace{\eta_t \langle \nabla F(w_{t-1}), \mathbb{E} \sum_{k=1}^K \eta_\ell^{\tau_t} [-\nabla F(w_k^{\tau_t}) - \xi_k^{\tau_t} - \eta_\ell^{\tau_t} H(w_k^{\tau_t})(w_{t-1} - w_{\tau_t}) + \nabla F(w_{t-1})] \rangle}_{T_{1,2}} \quad (194)$$

$$+ \frac{L \eta_\ell^2 \tilde{u}_t^2}{2}. \quad (195)$$

Here, B_1 admits the same control as the B_1 in Lemma 1 above. And A_1 above admits the same control as C_4 in Lemma 1 with a difference of η_t , we thus have

$$B_1 \leq G\eta_t \left[2^{\alpha-1}(\eta_\ell^{\tau_{C_t}})^\alpha \tilde{D}^\alpha + K^\alpha \eta_\ell^{2\alpha} 2^{3\alpha-3} (D^\alpha + D^\alpha)^2 (t - \tau_{C_t})^{\alpha-1} \sum_{i=\tau_{C_t}}^{t-1} \eta_i^\alpha \tilde{u}_i^\alpha \right]. \quad (196)$$

$$A_1 \leq G\eta_t \eta_\ell K d u_{\tau_{C_t}}^{1-\alpha} 2^{\alpha-1} (D^\alpha + D^\alpha). \quad (197)$$

Now, we will bound $T_{1,1}$:

$$T_{1,1} \leq \eta_t G \left\| \sum_{k=1}^K (\eta_\ell^{\tau_t})^2 \mathbb{E}[(\tilde{g}_k^{\tau_t})^{\odot 2} \mp (g_k^{\tau_t})^{\odot 2}] \odot (w_{t-1} - w_{\tau_t}) \mp (\text{Diag}(H(w_k^{\tau_t})) - H(w_k^{\tau_t}))(w_{t-1} - w_{\tau_t}) \right\| \quad (198)$$

$$\leq \eta_t G \sum_{k=1}^K (\eta_\ell^{\tau_t})^2 (\|\mathbb{E}[(\tilde{g}_k^{\tau_t})^{\odot 2} - (g_k^{\tau_t})^{\odot 2}]\| \|w_{t-1} - w_{\tau_t}\| + \|\mathbb{E}[(g_k^{\tau_t})^{\odot 2} - \text{Diag}(H(w_k^{\tau_t}))]\| \|w_{t-1} - w_{\tau_t}\|) \quad (199)$$

$$+ \|\mathbb{E}(\text{Diag}(H(w_k^{\tau_t})) - H(w_k^{\tau_t}))\| \|w_{t-1} - w_{\tau_t}\| \quad (200)$$

Now, we notice that for every coordinate, we have

$$\|\mathbb{E}[\text{Clip}(u_{\tau_t}, (\nabla F(x_k^{\tau_t}) + \xi_k^{\tau_t})_i)^2 - (\nabla F(x_k^{\tau_t}) + \xi_k^{\tau_t})_i^2]\| \quad (201)$$

$$\leq \mathbb{E}[\chi((\nabla F(x_k^{\tau_t}) + \xi_k^{\tau_t})_i > u_{\tau_t}) |u_{\tau_t}^2 - (\nabla F(x_k^{\tau_t}) + \xi_k^{\tau_t})_i^2|] \quad (202)$$

$$\leq \mathbb{E}[\chi((\nabla F(x_k^{\tau_t}) + \xi_k^{\tau_t})_i > u_{\tau_t}) |(\nabla F(x_k^{\tau_t}) + \xi_k^{\tau_t})_i|^{2\alpha} |(\nabla F(x_k^{\tau_t}) + \xi_k^{\tau_t})_i|^{2-2\alpha}] \quad (203)$$

$$\leq B^{2\alpha} u_{\tau_t}^{2-2\alpha}. \quad (204)$$

And this gives us that

$$\|\mathbb{E}[(\tilde{g}_k^{\tau_t})^{\odot 2} - (g_k^{\tau_t})^{\odot 2}]\| \leq dB^{2\alpha} u_{\tau_t}^{2-2\alpha} \quad (205)$$

Incorporating this bound, the assumption, and Lemma 1 into Eq. (200), we have that

$$T_{1,1} \leq \eta_t G \sum_{k=1}^K (\eta_\ell^{\tau_t})^2 (dB^{2\alpha} u_{\tau_t}^{2-2\alpha} + O(T^{\nu+\zeta})) \quad (206)$$

$$+ O(T^{\frac{(\alpha-1)\nu}{2}} + \tau^{\frac{\alpha}{2}} T^{\frac{(2\alpha-1)\nu+\alpha\omega+\alpha\zeta}{2}} + T^{\frac{\nu+\zeta}{2}} + \tau^{\frac{1}{2}} T^{\frac{\omega+\zeta}{2}} + \tau^{\frac{1}{2}} T^{\frac{2\zeta+\omega+\zeta+\nu}{2}} + T^{\frac{(1-\alpha)\zeta}{2}}) \quad (207)$$

$$+ T^{\frac{\omega-\nu+2\zeta}{2}} + \epsilon_{nc} + \epsilon_D) \|w_{t-1} - w_{\tau_t}\| \quad (208)$$

$$\leq \eta_t G \sum_{k=1}^K (\eta_\ell^{\tau_t})^2 (dB^{2\alpha} u_{\tau_t}^{2-2\alpha} + O(T^{\nu+\zeta})) \quad (209)$$

$$+ O(T^{\frac{(\alpha-1)\nu}{2}} + \tau^{\frac{2\alpha}{2}} T^{\frac{(\alpha-1)\nu+\alpha\omega+\alpha\zeta}{2}} + T^{\frac{\nu+\zeta}{2}} + \tau^{\frac{1}{2}} T^{\frac{\omega+\zeta}{2}} + \tau^{\frac{1}{2}} T^{\frac{2\zeta+\omega+\zeta+\nu}{2}} + T^{\frac{(1-\alpha)\zeta}{2}}) \quad (210)$$

$$+ T^{\frac{\omega-\nu+2\zeta}{2}} + \epsilon_{nc} + \epsilon_D) \sum_{i=\tau_t}^{t-1} \eta_i \tilde{u}_i. \quad (211)$$

Now, it remains to bound $T_{1,2}$:

$$T_{1,2} \leq \eta_t G \sum_{k=1}^K \eta_\ell^{\tau_t} (\|\nabla F(w_{t-1}) - \nabla F(w_k^{\tau_t}) - \eta_\ell H(w_k^{\tau_t})(w_{t-1} - w_{\tau_t})\|) \quad (212)$$

$$\leq \eta_t G \sum_{k=1}^K \eta_\ell^{\tau_t} (\|\nabla F(w_{t-1}) - \nabla F(w_k^{\tau_t}) \pm \nabla F(w_{\tau_t}) \pm \eta_\ell H(w_{\tau_t})(w_{t-1} - w_{\tau_t}) - \eta_\ell H(w_k^{\tau_t})(w_{t-1} - w_{\tau_t})\|) \quad (213)$$

$$\leq \eta_t G \sum_{k=1}^K \eta_\ell^{\tau_t} (\|\nabla F(w_{\tau_t}) - \nabla F(w_k^{\tau_t})\| + \|\nabla F(w_{t-1}) - [H(w_{\tau_t})(w_{t-1} - w_{\tau_t}) + \nabla F(w_{\tau_t})]\|) \quad (214)$$

$$+ \|\eta_\ell (H(w_{\tau_t}) - H(w_k^{\tau_t}))(w_{t-1} - w_{\tau_t})\| \quad (215)$$

$$\leq \eta_t G \sum_{k=1}^K \eta_\ell^{\tau_t} (L \sum_{i=0}^{k-1} \|w_{i+1}^{\tau_t} - w_i^{\tau_t}\| + \frac{L'}{2} (\sum_{i=\tau_t}^{t-1} \|w_i - w_{i-1}\|)^2 + |1 - \eta_\ell| (\sum_{i=\tau_t}^{t-1} \|w_i - w_{i-1}\|)) \quad (216)$$

$$+ 2\eta_\ell L' \|w_{t-1} - w_k^{\tau_t}\|^2) \quad (217)$$

$$\leq \eta_t G \sum_{k=1}^K \eta_\ell^{\tau_t} \left(L \sum_{i=0}^{k-1} \sqrt{du_{\tau_t}} \eta_\ell^{\tau_t} + \frac{L'}{2} (\sum_{i=\tau_t}^{t-1} \eta_i \tilde{u}_i)^2 + |1 - \eta_\ell| (\sum_{i=\tau_t}^{t-1} \eta_i \tilde{u}_i) + 2\eta_\ell L' (\sum_{i=0}^{k-1} \sqrt{du_{\tau_t}} \eta_\ell^{\tau_t} + \sum_{i=\tau_t}^{t-1} \eta_i \tilde{u}_i)^2 \right) \quad (218)$$

Now, we can combine the bounds together and get

$$K \eta_t \eta_\ell^{\tau_t} \|\nabla F(w_{t-1})\|^2 \quad (219)$$

$$\leq F(w_{t-1}) - \mathbb{E}F(w_t) + 2^{\alpha-1} G \bar{D}^\alpha \eta_t (\eta_\ell^{\tau_t})^\alpha + G \eta_t K^\alpha \eta_\ell^{2\alpha} 2^{3\alpha-3} (D^\alpha + D^\alpha)^2 (t - \tau_{C_t})^{\alpha-1} \sum_{i=\tau_{C_t}}^{t-1} \eta_i^\alpha \tilde{u}_i^\alpha \quad (220)$$

$$+ G \eta_t \eta_\ell K d u_{\tau_{C_t}}^{1-\alpha} 2^{\alpha-1} (D^\alpha + D^\alpha) + \frac{L \eta^2 \tilde{u}_t^2}{2} + \eta_t G \sum_{k=1}^K (\eta_\ell^{\tau_t})^2 [dB^{2\alpha} u_{\tau_t}^{2-2\alpha} + O(T^{\nu+\zeta} + T^{\frac{(\alpha-1)\nu}{2}})] \quad (221)$$

$$+ O\left(\tau^{\frac{\alpha}{2}} T^{\frac{(2\alpha-1)\nu+\alpha\omega+\alpha\tilde{\zeta}}{2}} + T^{\frac{\nu+\zeta}{2}} + \tau^{\frac{1}{2}} T^{\frac{\omega+\tilde{\zeta}}{2}} + \tau^{\frac{1}{2}} T^{\frac{2\zeta+\omega+\tilde{\zeta}+\nu}{2}} + T^{\frac{(1-\alpha)\zeta}{2}} + T^{\frac{\omega-\nu+2\tilde{\zeta}}{2}}\right) + \epsilon_{nc} + \epsilon_D] \sum_{i=\tau_t}^{t-1} \eta_i \tilde{u}_i \quad (222)$$

$$+ \eta_t G \sum_{k=1}^K \eta_\ell^{\tau_t} \left(L \sum_{i=0}^{k-1} \sqrt{du_{\tau_t}} \eta_\ell^{\tau_t} + \frac{L'}{2} (\sum_{i=\tau_t}^{t-1} \eta_i \tilde{u}_i)^2 + |1 - \eta_\ell| (\sum_{i=\tau_t}^{t-1} \eta_i \tilde{u}_i) + 2\eta_\ell L' (\sum_{i=0}^{k-1} \sqrt{du_{\tau_t}} \eta_\ell^{\tau_t} + \sum_{i=\tau_t}^{t-1} \eta_i \tilde{u}_i)^2 \right) \quad (223)$$

And by telescoping, we have that

$$\Omega(T^{\omega+\nu+1}) \min_{t \in [T]} \|\nabla F(w_{t-1})\|^2 \quad (224)$$

$$\leq O(1 + T^{\omega+\alpha\nu+1} + \tau^\alpha T^{(\alpha+1)\omega+2\alpha\nu+\alpha\tilde{\zeta}+1} + T^{\nu+\omega+(1-\alpha)\zeta+1} + T^{2\omega+2\tilde{\zeta}+1} + \tau T^{(2-2\alpha)\zeta+\tilde{\zeta}+2\omega+2\nu+1}) \quad (225)$$

$$+ \tau T^{2\omega+3\nu+\zeta+\tilde{\zeta}+1} + \tau T^{2\omega+\frac{(\alpha+3)\nu}{2}+\tilde{\zeta}+1} + \tau^{\frac{\alpha}{2}+1} T^{\frac{(2\alpha+3)\nu}{2}+(2+\frac{\alpha}{2})\omega+(1+\frac{\alpha}{2})\tilde{\zeta}+1} + \tau T^{\frac{5\nu+\zeta}{2}+2\omega+\tilde{\zeta}+1} \quad (226)$$

$$+ \tau^{\frac{3}{2}} T^{\frac{5\omega}{2}+\zeta+\frac{3}{2}\tilde{\zeta}+\frac{5\nu}{2}+1} + \tau T^{2\omega+2\nu+\tilde{\zeta}+\frac{(1-\alpha)\zeta}{2}+1} + \tau T^{\frac{5\omega+3\nu+4\tilde{\zeta}}{2}+1} + \tau T^{2\omega+2\nu+\tilde{\zeta}+1} + T^{2\nu+\omega+\zeta+1} \quad (227)$$

$$+ \tau^2 T^{3\omega+\nu+2\tilde{\zeta}+1} + \tau T^{2\omega+\nu+\tilde{\zeta}+1} + T^{4\nu+\omega+2\zeta+1} + \tau^2 T^{3\omega+2\nu+2\tilde{\zeta}+1}) \quad (228)$$

$$\leq O(1 + T^{\omega+\alpha\nu+1} + \tau^\alpha T^{(\alpha+1)\omega+2\alpha\nu+\alpha\tilde{\zeta}+1} + T^{\nu+\omega+(1-\alpha)\zeta+1} + T^{2\omega+2\tilde{\zeta}+1} + \tau T^{(2-2\alpha)\zeta+\tilde{\zeta}+2\omega+2\nu+1}) \quad (229)$$

$$+ \tau T^{2\omega+3\nu+\zeta+\tilde{\zeta}+1} + \tau T^{2\omega+\frac{(\alpha+3)\nu}{2}+\tilde{\zeta}+1} + \tau^{\frac{\alpha}{2}+1} T^{\frac{(2\alpha+3)\nu}{2}+(2+\frac{\alpha}{2})\omega+(1+\frac{\alpha}{2})\tilde{\zeta}+1} + \tau T^{\frac{5\nu+\zeta}{2}+2\omega+\tilde{\zeta}+1} \quad (230)$$

$$+ \tau^{\frac{3}{2}} T^{\frac{2\zeta+5\omega+5\nu+3\tilde{\zeta}}{2}+1} + \tau T^{\frac{5\omega+3\nu+4\tilde{\zeta}}{2}+1} + T^{2\nu+\omega+\zeta+1} + \tau T^{2\omega+\nu+\tilde{\zeta}+1} + \tau^2 T^{3\omega+\nu+2\tilde{\zeta}+1} + \tau T^{2\omega+\nu+\tilde{\zeta}+1} \quad (231)$$

$$+ T^{4\nu+\omega+2\zeta+1}). \quad (232)$$

And moving the LHS to the RHS proves the theorem. \square

C. Experiment Details

In this section, we will explain the detailed setup of our experiments across three different tasks: image classification task with ViT on CIFAR-10, and natural language processing task with pre-trained BERT model on GLUE. Throughout our experiments, we will use simulated runtime for different clients. Before each global training round, each client samples a runtime from a fixed distribution out of three types: small (runtime:1-2), medium (runtime: 3-5), and large. The large runtime distribution depends on the straggler mode. If the straggler mode is ‘large’, then the large runtime distribution corresponds to a runtime in the range 20-40, which corresponds to scenarios where there are large stragglers. Otherwise, the straggler mode is ‘mild’, and the large runtime distribution corresponds to a runtime in the range 5-8. All the experiments are conducted on 5 GPU servers with L40s machines.

C.1. Image Classification Task with CIFAR-10

We evaluate our method using the Vision Transformer (ViT), a model for image recognition developed by Google Research. ViT directly applies the standard Transformer architecture. It processes an image by splitting it into a sequence of fixed-size patches, making it a highly effective model for classification and an excellent baseline for evaluating our methods.

To evaluate image classification performance, we utilize the CIFAR-10 dataset, a widely recognized benchmark for computer vision research. Specifically, we fine-tune a pre-trained ViT model on the CIFAR-10 training set. The dataset consists of 60,000 32x32 color images distributed across 10 classes, including airplane, automobile, bird, and cat. These images present a diverse set of objects and backgrounds, providing a robust evaluation of a model’s ability to learn core visual features and generalize effectively.

The experiments are conducted with $N = 40$ clients, in which 17 of them sample runtime from the small runtime distribution, 12 of them sample runtime from the medium runtime distribution, and the remaining 11 of them sample runtime from the large runtime distribution. We use $K = 5$ client-side epochs, and $T = 140$ global epochs. The range of M that we explore is $\{1, 4, 10\}$. The *Clip* that we use is coordinate-wise upper-clipping. The server/client-side learning rates, server/client-side clipping thresholds are determined by the hyperparameter sweep laid out in Appendix C.3 for different server-side and client-side optimizers.

C.2. Natural Language Processing Task with GLUE

We evaluate the proposed method using the RoBERTa model, an encoder-only architecture derived from BERT. To rigorously assess natural language understanding capabilities, we employ the General Language Understanding Evaluation (GLUE) benchmark, a widely adopted suite of datasets for the training, evaluation, and analysis of natural language processing systems. GLUE comprises a diverse range of tasks, including sentiment classification, semantic textual similarity, textual entailment, and natural language inference, thereby offering a comprehensive assessment of model performance across multiple linguistic dimensions. For all experiments, we adhere to standard RoBERTa fine-tuning protocols, initializing with pretrained weights and optimizing task-specific objectives for each dataset within the benchmark.

The experiments are conducted with $N = 10$, $M = 4$, $K = 1$ client-side epochs, and a maximum of $T = 30$ global epochs. The clipping operation (*Clip*) employed is coordinate-wise upper-clipping. The server- and client-side learning rates, along with the corresponding clipping thresholds, are specified in Appendix C.3 for different server-side and client-side optimizers. To demonstrate the applicability of our methods to few-shot/many-shot settings, we follow prior work (Gao et al., 2020; Raman et al., 2023; Malladi et al., 2023) and sub-sample the training samples for tasks QQP, MNLI, QNLI, and SST-2 to 5,000 samples each. For STS-B, we report the Pearson correlation coefficient scaled to the range $[0,1]$, while for the remaining tasks we report accuracy.

C.3. Hyperparameter Sweep and Optimal Hyperparameters

For each experiment, we use a hyperparameter sweep grid to find the hyperparameter choice that gives the best result. We first present the hyperparameter sweep grid that we used for different algorithms and settings in Table 4.

It should be noticed that due to time constraints, we only conduct the complete hyperparameter sweep for Sync-*Clip*² for each straggler mode. For the remaining *Clip*² experiments with the same straggler mode, we use the same optimal server-side and client-side upper clipping threshold obtained by the hyperparameter sweep of Sync-*Clip*² under the same straggler mode, given that the magnitude of the gradients is relatively stable under the same straggler mode.

Asynchronous Heavy-Tailed Optimization

Algorithm	Server-side LR	Client-side LR	Server-side U	Client-side U
SGDClip	(0.1, 0.01, 0.001, 0.0001)	(0.1, 0.01, 0.001, 0.0001)	-	np.linspace(10^{-4} , 1.5, 4)
<i>Clip</i> ²	(0.1, 0.01, 0.001, 0.0001)	(0.1, 0.01, 0.001, 0.0001)	np.linspace(10^{-4} , 1.5, 4)	np.linspace(10^{-4} , 1.5, 4)
SD-SGDClip	(0.1, 0.01, 0.001, 0.0001)	(0.1, 0.01, 0.001, 0.0001)	-	np.linspace(10^{-4} , 1.5, 4)
SD- <i>Clip</i> ²	(0.1, 0.01, 0.001, 0.0001)	(0.1, 0.01, 0.001, 0.0001)	np.linspace(10^{-4} , 1.5, 4)	np.linspace(10^{-4} , 1.5, 4)
DC-SGDClip	(0.1, 0.01, 0.001, 0.0001)	(0.1, 0.01, 0.001, 0.0001)	-	np.linspace(10^{-4} , 1.5, 4)
DC- <i>Clip</i> ²	(0.1, 0.01, 0.001, 0.0001)	(0.1, 0.01, 0.001, 0.0001)	np.linspace(10^{-4} , 1.5, 4)	np.linspace(10^{-4} , 1.5, 4)

Table 4. Hyperparameter sweep grids.

Table 5 below gives the optimal hyperparameters for all experiments over CIFAR-10.

Algorithm	Straggler mode	Server-side LR	Client-side LR	Server-side U	Client-side U
Sync SGDClip	large	0.0001	0.01	-	0.0001
Sync SGDClip	mild	0.0001	0.01	-	1.0
SC Async SGDClip	large	0.0001	0.0001	-	0.5
SC Async SGDClip	mild	0.0001	0.01	-	1.0
CC Async SGDClip	large	0.0001	0.0001	-	0.5
CC Async SGDClip	mild	0.0001	0.001	-	0.5
SC SD SGDClip	large	0.01	0.1	-	0.5
SC SD SGDClip	mild	0.01	0.1	-	1.0
CC SD SGDClip	large	0.01	0.01	-	1.0
CC SD SGDClip	mild	0.01	0.001	-	1.5
Sync <i>Clip</i> ²	large	0.01	0.1	1.0	0.5
Sync <i>Clip</i> ²	mild	0.01	0.1	1.5	1.5
SC Async <i>Clip</i> ²	large	0.1	0.01	1.0	0.5
SC Async <i>Clip</i> ²	mild	0.1	0.01	1.5	1.5
CC Async <i>Clip</i> ²	large	0.1	0.01	1.0	0.5
CC Async <i>Clip</i> ²	mild	0.01	0.1	1.5	1.5
SC SD <i>Clip</i> ²	large	0.1	0.01	1.0	0.5
SC SD <i>Clip</i> ²	mild	0.1	0.01	1.5	1.5
CC SD <i>Clip</i> ²	large	0.1	0.01	1.0	0.5
CC SD <i>Clip</i> ²	mild	0.1	0.01	1.5	1.5
SC DC <i>Clip</i> ²	large	0.1	0.01	1.5	1.5
SC DC <i>Clip</i> ²	mild	0.1	0.01	0.5	1.0
CC DC <i>Clip</i> ²	large	0.1	0.01	1.5	1.5
CC DC <i>Clip</i> ²	mild	0.1	0.01	0.5	1.0

Table 5. Optimal Hyperparameters for experiments on CIFAR-10.

Table 6 and Table 7 give the optimal hyperparameters for all experiments over GLUE Benchmark.

D. Experimental Results

In this section, we present all the specific result tables of the experiments mentioned in Section 5. The accuracies are the best accuracies obtained during the sweep of hyperparameters.

D.1. Accuracies and Runtime Across Different Methods for CIFAR-10

Please see results in Table 8-Table 12.

For baseline comparison results presented in 12, we try our best to tune hyperparameters for the baseline methods. E.g., for

Asynchronous Heavy-Tailed Optimization

Dataset	Algorithm	Straggler mode	Server-side LR	Client-side LR	Server-side U	Client-side U
MNLI	SGDClip	mild&large	1	0.56	-	0.0001
	Sync <i>Clip</i> ²	mild&large	1	0.5	0.75	0.0001
	Async <i>Clip</i> ²	mild&large	1	0.5	1	0.0001
QQP	SGDClip	mild&large	1	0.56	-	0.0001
	<i>Clip</i> ²	mild&large	1	0.5	1.5	0.0001
	SGDClip	mild&large	1	0.5	-	0.0001
	Sync <i>Clip</i> ²	mild&large	1	0.1	0.01	0.0001
	SC Async <i>Clip</i> ²	mild&large	0.1	0.1	0.01	0.0001
	CC Async <i>Clip</i> ²	mild&large	1	1	10.0	0.0001
	SC SD <i>Clip</i> ²	mild&large	0.5	0.5	0.0001	0.0001
	CC SD <i>Clip</i> ²	mild&large	1	1	10.0	0.0001
	SC DC <i>Clip</i> ²	mild&large	0.5	0.5	0.01	0.0001
CC DC <i>Clip</i> ²	mild&large	1	1	10.0	0.0001	
SST-2	SGDClip	mild&large	1	0.56	-	0.0001
	Sync <i>Clip</i> ²	large	1	0.5	0.001	0.0001
	Sync <i>Clip</i> ²	mild	1	0.5	0.0001	0.0001
	Async <i>Clip</i> ²	mild&large	1	0.5	0.75	0.0001
SST-B	SGDClip	mild&large	1	0.44	-	0.0001
	<i>Clip</i> ²	mild&large	0.5	0.5	0.0001	0.0001

Table 6. Optimal Hyper-parameters for task: MNLI, QQP, RTE, SST-2 and SST-B in the GLUE benchmark.

FADAS, we tune client- and server-side learning rates from (0.1, 0.01, 0.001, 0.0001) and the delay threshold in their paper τ_c from (1, 4, 8, 10). For DN-DyLU, we tune learning rates in the same way and N from (4, 8, 16).

D.2. Effects of M

To explore the effect of M for different methods, we run the image classification experiment on the dataset CIFAR-10 with $M \in \{1, 10, 20, 30\}$ using the optimal hyperparameters determined by the sweep explained in Appendix C.3 when $M = 4$. Notice that in general there is no clear dominance of server-centric or client-centric regimes over the other, so we run the server-centric version for asynchronous methods. The results are presented in Table 13.

Notably, we see that non-synchronous *SGDClip* with both large and mild stragglers give significantly lower accuracies (10.3 and 9.8) when $M = 1$. We believe stem from interplays between heavy-tailed noise and asynchrony: When $M = 1$, the server updates its parameter whenever a client sends its results back, and the server immediately sends its updated parameters to that client to start a new round of local updates. This can be detrimental when the server receives delayed updates from an extreme straggler, which comes from an old model that is drastically different from the current global model. In the meantime, fast clients will more frequently update the model. Therefore, the negative effect of the delayed updates from stragglers is exaggerated compared to a larger M , thus causing the model to not converge, especially with the existence of heavy-tailed noise. We see that both server-side clipping and simply using synchronous training effectively address the problem of low accuracy. This suggests that our proposed stateless-aware aggregation method would achieve better performance when used together with *Clip*² than *SGDClip*, in extreme asynchronous cases.

D.3. Additional Results

Please see Figure 5 which shows the loss/epochs and loss/runtime tradeoffs on the mild straggler setting on the CIFAR-10 dataset.

D.4. Detailed Experiment Results over Each Task in GLUE Benchmark

In this section, we report the experimental results on the GLUE benchmark for each individual task. Specifically, we evaluate three settings: (21 synchronous and asynchronous fine-tuning without staleness-aware downplaying or delay compensation (Table 14); (3) fine-tuning with staleness-aware downplaying86.0 (Table 15); and (3) fine-tuning with delay compensation (Table 16).

Asynchronous Heavy-Tailed Optimization

Dataset	Algorithm	Straggler mode	Server-side LR	Client-side LR	Server-side U	Client-side U
QNLI	Sync SGDClip	mild&large	1	0.44	-	0.0001
	Async SGDClip	mild&large	1	0.5	-	0.0001
	Sync $Clip^2$	large	0.5	0.5	0.001	0.0001
	Sync $Clip^2$	mild	1	0.5	0.01	0.0001
	SC Async $Clip^2$	large	0.5	0.5	0.001	0.0001
	SC Async $Clip^2$	mild	0.5	0.5	0.01	0.0001
	CC Async $Clip^2$	mild&large	1	0.5	0.0001	0.0001
	SC SD $Clip^2$	large	1	0.5	0.001	0.0001
	SC SD $Clip^2$	mild	1	0.5	0.0001	0.0001
	CC SD $Clip^2$	mild&large	1	0.5	0.0001	0.0001
	SC DC $Clip^2$	large	0.5	0.5	0.001	0.0001
	SC DC $Clip^2$	mild	0.5	0.5	0.01	0.0001
	CC DC $Clip^2$	mild&large	1	0.5	0.0001	0.0001
	MRPC	Sync SGDClip	mild&large	1	0.89	-
SC Async SGDClip		mild&large	1	1	-	0.0001
CC Async SGDClip		mild&large	1	0.89	-	0.0001
SC SD SGDClip		mild&large	1	1	-	0.0001
CC SD SGDClip		mild&large	1	0.89	-	0.0001
Sync $Clip^2$		large	1	1	0.0001	0.0001
Sync $Clip^2$		mild	0.5	1	0.001	0.0001
SC Async $Clip^2$		mild&large	1	1	0.01	0.0001
CC Async $Clip^2$		mild&large	1	1	0.0001	0.0001
SC SD $Clip^2$		mild&large	1	1	0.001	0.0001
CC SD $Clip^2$		mild&large	1	1	0.0001	0.0001
SC DC $Clip^2$		large	1	1	0.01	0.0001
SC DC $Clip^2$		mild	0.5	1	0.01	0.0001
CC DC $Clip^2$		mild&large	1	1	0.0001	0.0001
CoLA	Sync SGDClip	mild&large	1	0.89	-	0.0001
	Async SGDClip	mild&large	1	0.5	-	0.0001
	Sync $Clip^2$	large	1	0.5	0.01	0.0001
	Sync $Clip^2$	mild	1	0.5	0.001	0.0001
	SC Async $Clip^2$	large	1	0.5	0.001	0.0001
	SC Async $Clip^2$	mild	1	0.5	0.0001	0.0001
	CC Async $Clip^2$	mild&large	1	0.5	0.75	0.0001
	SC SD $Clip^2$	large	0.5	0.5	0.01	0.0001
	SC SD $Clip^2$	mild	0.5	0.5	0.001	0.0001
	CC SD $Clip^2$	mild&large	1	0.5	0.75	0.0001
	SC DC $Clip^2$	large	1	0.5	0.0001	0.0001
	SC DC $Clip^2$	mild	0.5	0.5	0.001	0.0001
	CC DC $Clip^2$	mild&large	1	0.5	0.75	0.0001

Table 7. Optimal Hyperparameters for task QNLI, MRPC, and CoLA on GLUE benchmark.

Again, for FADAS in Table 17, we try our best to tune hyperparameters: we tune client- and server-side learning rates from (0.1, 0.01, 0.001, 0.0001) and the delay threshold in their paper τ_c from (1, 4, 8, 10).

Methods	CIFAR-10		GLUE	
	Acc.	runtime	Acc.	runtime
Sync SGDClip (mild straggler)	98.6	818	82.5	93
Server-centric Async SGDClip (mild straggler)	97.7	40	83.4	21
Client-centric Async SGDClip (mild straggler)	98.4	36	83.0	20
Sync SGDClip (large straggler)	98.6	3170	82.5	445
Server-centric Async SGDClip (large straggler)	97.7	44	82.2	36
Client-centric Async SGDClip (large straggler)	97.9	40	83.4	26

Table 8. Best accuracy and runtime comparisons of Sync SGDClip and Async SGDClip. Asynchronous training achieves similar test performance compared with the synchronous case but requires much less runtime.

Methods	CIFAR-10		GLUE	
	Acc.	runtime	Acc.	runtime
Sync $Clip^2$ (mild straggler)	98.4	860	82.7	95
Server-centric Async $Clip^2$ (mild straggler)	98.3	40	82.9	23
Client-centric Async $Clip^2$ (mild straggler)	98.1	37	83.9	26
Sync $Clip^2$ (large straggler)	98.4	3139	82.6	380
Server-centric Async $Clip^2$ (large straggler)	98.2	42	82.0	21
Client-centric Async $Clip^2$ (large straggler)	98.3	39	83.3	31

Table 9. Best accuracy and runtime comparisons of synchronous $Clip^2$ and asynchronous $Clip^2$. Asynchronous training achieves similar test performance compared with the synchronous case but requires much less runtime.

Async Mode	Methods	CIFAR-10		GLUE	
		Acc.	runtime	Acc.	runtime
Server-centric	SGDClip (mild straggler)	97.7	40	83.4	21
	SD-SGDClip (mild straggler)	98.2	41	82.0	24
	SGDClip (large straggler)	97.7	44	82.2	36
	SD-SGDClip (large straggler)	98.2	44	81.9	22
Client-centric	SGDClip (mild straggler)	98.4	36	83.0	20
	SD-SGDClip (mild straggler)	98.2	36	82.3	17
	SGDClip (large straggler)	97.9	40	83.4	26
	SD-SGDClip (large straggler)	98.0	39	82.8	30

Table 10. Best accuracy and runtime comparisons of Async SGDClip and Async SD-SGDClip (i.e., SGDClip with staleness-aware downplaying).

Asynchronous Heavy-Tailed Optimization

Async Mode	Methods	CIFAR-10		GLUE	
		Acc.	runtime	Acc.	runtime
Server-centric	<i>Clip</i> ² (mild straggler)	98.3	40	82.9	23
	SD-Clip ² (mild straggler)	98.2	39	82.7	22
	DC-Clip ² (mild straggler)	98.4	42	81.8	24
	<i>Clip</i> ² (large straggler)	98.2	42	82.0	21
	SD-Clip ² (large straggler)	98.2	43	81.6	18
	DC-Clip ² (large straggler)	98.5	45	81.5	25
Client-centric	<i>Clip</i> ² (mild straggler)	98.1	37	83.9	26
	SD-Clip ² (mild straggler)	98.0	37	82.7	23
	DC-Clip ² (mild straggler)	98.3	36	84.3	33
	<i>Clip</i> ² (large straggler)	98.3	39	83.3	31
	SD-Clip ² (large straggler)	97.9	39	84.3	41
	DC-Clip ² (large straggler)	98.3	39	83.4	90

Table 11. Best Accuracy and Runtime comparisons of Async *Clip*², Async SD-*Clip*², and Async DC-*Clip*².

Async Mode	Methods	Acc.
Server-centric	<i>Clip</i> ² (mild straggler)	98.3
	SD-Clip ² (mild straggler)	98.2
	DC-Clip ² (mild straggler)	98.4
	<i>Clip</i> ² (large straggler)	98.2
	SD-Clip ² (large straggler)	98.2
	DC-Clip ² (large straggler)	98.5
Client-centric	<i>Clip</i> ² (mild straggler)	98.1
	SD-Clip ² (mild straggler)	98.0
	DC-Clip ² (mild straggler)	98.3
	<i>Clip</i> ² (large straggler)	98.3
	SD-Clip ² (large straggler)	97.9
	DC-Clip ² (large straggler)	98.3
N/A	FADAS (Wang et al., 2024a) (mild straggler)	93.5
N/A	FADAS (Wang et al., 2024a) (large straggler)	94.3
N/A	DN+DyLU (Liu et al., 2024) (mild straggler)	97.3
N/A	DN+DyLU (Liu et al., 2024) (large straggler)	97.5

Table 12. Accuracies (in %) Comparison for (SD/DC-)Clip² with FADAS and DN+DyLU on CIFAR-10.

Algorithm	Straggler	M=1 Acc.	M=1 Runtime	M=10 Acc.	M=10 Runtime	M=20 Acc.	M=20 Runtime	M=30 Acc.	M=30 Runtime
Sync SGDClip	large	97.4	1328	97.0	4715	97.0	5163	96.9	5393
Async SGDClip	large	10.3	10	97.3	115	97.5	289	97.7	832
SD SGDClip	large	10.3	12	97.4	122	97.7	291	97.8	869
Sync SGDClip	mild	96.8	559	98.5	1036	98.3	1081	98.4	1090
Async SGDClip	mild	9.8	11	98.3	104	98.5	248	98.4	541
SD SGDClip	mild	9.8	12	97.1	98	97.6	248	97.9	541
Sync <i>Clip</i> ²	large	94.6	1424	94.5	4645	95.0	5447	95.0	5420
Async <i>Clip</i> ²	large	97.5	14	98.2	117	98.3	282	98.3	824
SD <i>Clip</i> ²	large	98.0	12	98.0	119	98.2	285	98.4	813
Sync <i>Clip</i> ²	mild	93.6	489	95.1	1027	94.8	1096	94.9	1100
Async <i>Clip</i> ²	mild	97.8	12	98.4	99	98.4	247	98.5	538
SD <i>Clip</i> ²	mild	92.4	11	79.5	101	98.1	244	98.5	538
DC <i>Clip</i> ²	large	98.0	11	98.3	115	-	-	-	-
DC <i>Clip</i> ²	mild	97.7	10	98.0	102	98.2	249	98.2	544

Table 13. Accuracies (in %) and runtimes for different M values on CIFAR-10.

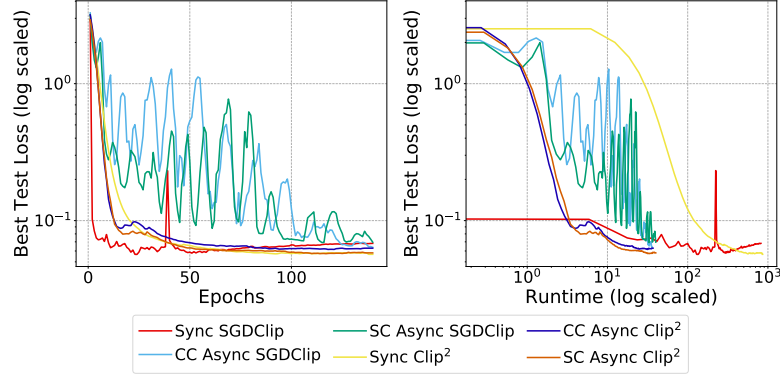


Figure 5. Best Test Loss v.s. Epochs and Runtime of Sync SGDClip/ $Clip^2$ and Async SGDClip/ $Clip^2$ under the mild straggler setting on CIFAR-10.

Mode		MNLI		QNLI		QQP		RTE		SST-2		MPRC		CoLA		STS-B		
Algorithm	Straggler	Acc.	Runtime	Acc.	Runtime	Acc.	Runtime	Acc.	Runtime	Acc.	Runtime	Acc.	Runtime	Acc.	Runtime	Pearson	Runtime	
SGDClip	Mild	Sync.	83.15	96	86.58	102	86.98	96	57.76	105	91.86	88	84.80	94	81.11	63	87.32	103
		Server	82.50	19	84.72	18	86.33	23	69.26	26	92.09	16	82.11	24	81.59	19	88.92	22
		Client	82.18	19	86.91	18	81.91	15	70.04	16	91.51	18	82.35	32	80.15	23	89.33	19
	Large	Sync.	82.88	451	86.53	510	86.92	509	63.18	443	92.20	516	83.58	303	81.21	369	83.65	457
		Server	82.58	21	85.78	22	86.09	16	60.29	16	91.97	17	80.39	19	81.69	31	88.42	26
		Client	82.21	21	87.48	27	85.03	27	70.07	16	90.94	12	82.60	70	80.35	23	88.22	13
$Clip^2$	Mild	Sync.	83.67	97	87.44	88	79.86	86	64.30	104	92.88	95	86.03	87	82.08	105	86.54	99
		Server	83.54	28	84.72	18	86.33	23	60.29	26	92.66	22	86.03	16	81.11	26	88.14	22
		Client	81.87	31	86.86	35	85.37	20	70.04	27	91.63	14	87.01	18	81.02	23	87.15	40
	Large	Sync.	83.30	419	87.22	511	83.03	406	64.30	480	92.78	422	85.05	281	79.77	58	86.43	461
		Server	82.58	21	85.78	22	86.09	16	59.95	16	91.97	17	83.58	19	80.44	31	85.63	23
		Client	82.19	14	86.89	22	85.39	41	67.87	45	92.29	69	85.05	19	80.15	23	86.92	17

Table 14. Accuracy and runtime comparison of synchronous, server-centric asynchronous, and client-centric asynchronous methods under SGDClip and $Clip^2$ optimizers, in settings with mild and large stragglers.

Mode		MNLI		QNLI		QQP		RTE		SST-2		MPRC		CoLA		STS-B		
Algorithm	Straggler	Acc.	Runtime	Acc.	Runtime	Acc.	Runtime	Acc.	Runtime	Acc.	Runtime	Acc.	Runtime	Acc.	Runtime	Pearson	Runtime	
SGDClip	Mild	Server	81.57	23	84.40	26	85.35	23	61.39	20	91.17	25	83.82	24	82.07	22	86.36	25
		Client	80.14	23	86.53	13	82.78	11	64.26	9	90.94	22	83.33	26	81.40	13	88.65	20
		Server	81.50	26	81.99	23	85.26	20	60.3	21	92.10	23	85.29	22	81.40	20	87.36	22
	Large	Client	82.20	14	87.42	43	84.43	13	63.90	13	91.17	25	83.58	33	81.02	28	88.46	68
		Server	82.18	21	87.24	26	84.48	17	64.32	21	93.11	20	82.11	20	80.47	22	87.33	25
		Client	83.42	14	86.91	20	86.10	37	70.76	30	92.20	39	85.78	13	80.35	20	86.19	13
$Clip^2$	Large	Server	82.50	19	87.59	14	84.47	21	54.51	23	92.78	15	84.31	17	81.40	15	85.60	21
		Client	83.35	16	86.55	55	86.96	40	72.56	74	91.51	65	86.52	18	80.73	38	86.60	21

Table 15. Accuracy and runtime comparison of synchronous, server-centric asynchronous, and client-centric asynchronous methods under SGDClip and $Clip^2$ optimizers, in settings with mild and large stragglers. We additionally leverage staleness-aware downplaying.

Mode		MNLI		QNLI		QQP		RTE		SST-2		MPRC		CoLA		STS-B		
Algorithm	Straggler	Acc.	Runtime	Acc.	Runtime	Acc.	Runtime	Acc.	Runtime	Acc.	Runtime	Acc.	Runtime	Acc.	Runtime	Pearson	Runtime	
$Clip^2$	Mild	Server	83.30	30	86.66	31	86.52	31	56.32	19	93.23	22	82.35	21	79.87	17	86.36	20
		Client	81.56	29	86.53	23	86.57	36	70.40	33	92.09	21	86.76	31	81.88	53	88.37	38
		Server	83.50	30	86.47	27	86.92	34	58.14	19	92.78	19	77.45	26	80.57	21	85.60	22
	Large	Client	82.29	23	86.36	36	84.44	59	66.43	48	91.63	25	86.03	42	81.78	370	87.91	113

Table 16. Accuracy and runtime comparison of synchronous, server-centric asynchronous, and client-centric asynchronous methods under SGDClip and $Clip^2$ optimizers, in settings with mild and large stragglers. We additionally leverage delay compensation.

Algorithm	Straggler	Async Mode	MNLI	QNLI	QQP	RTE	SST-2	MPRC	CoLA	STS-B	Avg
$Clip^2$	Large	Server	82.58	85.78	86.09	59.95	91.97	83.58	80.44	85.63	82.00
		Client	82.19	86.89	85.39	67.87	92.29	85.05	80.15	86.92	81.33
SD- $Clip^2$	Large	Server	82.50	87.59	84.47	54.51	92.78	84.31	81.40	85.60	81.65
		Client	83.35	86.55	86.96	72.56	91.51	86.52	80.73	86.60	84.35
DC- $Clip^2$	Large	Server	83.50	86.47	86.92	58.14	92.78	77.45	80.57	85.60	81.43
		Client	82.29	86.36	84.44	66.43	91.63	86.03	81.78	87.91	83.36
FADAS (Wang et al., 2024a)	Large	N/A	79.28	80.58	83.82	55.60	89.22	77.23	79.44	79.60	78.10

Table 17. Accuracy comparison between (SD/DC)- $Clip^2$ and FADAS.